SEDIMENTOLOGY AND STRATIGRAPHY OF MIOCENE-AGE GLACIAL DEPOSITS, FRIIS HILLS, ANTARCTICA

A Thesis
Submitted to the Graduate Faculty
of the
North Dakota State University
of Agriculture and Applied Science

By

Alexander Ryan Smith

In Partial Fulfillment of the Requirements
for the Degree of
MASTER OF SCIENCE

Major Program:
Environmental and Conservation Sciences

October 2011

Fargo, North Dakota

North Dakota State University
Graduate School

Title

Sedimentology and Stratigraphy of Miocene-Age Glacial Deposits,

Friis Hills, Antarctica

By

Alexander Ryan Smith

The Supervisory Committee certifies that this ***disquisition*** complies with North Dakota State University's regulations and meets the accepted standards for the degree of

MASTER OF SCIENCE

ABSTRACT

Smith, Alexander Ryan, M.S., Environmental and Conservation Science Program, College of Graduate and Interdisciplinary Studies, North Dakota State University, October 2011. Sedimentology and Stratigraphy of Miocene-age Glacial Deposits, Friis Hills, Antarctica. Major Professor: Dr. Adam Lewis.

The Friis Hills is an isolated plateau standing as much as 600 m above surrounding topography in the McMurdo Dry Valleys region of Antarctica. Preserved on the plateau surface is a sequence of early to middle Miocene-aged drifts. At the eastern edge of the plateau, these drifts fill a shallow paleovalley to a depth of at least 35 m. The drifts are exposed in a natural cross-section where modern topography crosscuts the paleovalley. Establishing an age and an environmental interpretation for these deposits is important because Antarctic paleoclimate records are lacking from the Mid-Miocene Climate Optimum.

Two drifts fill the ancient paleovalley in the eastern Friis Hills. The upper drift is here named Cavendish drift; the lower is here named Friis drift. Cavendish can be subdivided into three units, whereas Friis drift can be subdivided into two units. Each of these units is a horizontal bed that laps on paleovalley sidewalls. The lowest, Friis II, is a compact diamicton that is overlain by a nearly *in-situ*, bedded volcanic ash. Based on $^{40}Ar/^{39}Ar$ dating, the ash is 19.76 ± 0.07 Ma old. A second diamicton, Friis I, conformably blankets Friis II and was discovered to hold fossiliferous interbeds. Both Friis I and II contain erratic clasts and both are lodgement tills deposited from small, locally derived, alpine glaciers. Bedrock striations show ice flow to the northeast at azimuths between 025° to 032°, parallel to the trend of the paleovalley axis. Above these, Cavendish I, II, and III were deposited when thick ice covered the Friis Hills. Where the Cavendish drift laps onto

paleovalley sidewalls, bedrock striations show ice flow from 077° to 150°. Cavendish drift was deposited sometime after 19.8 Ma but before 14 Ma, when the Dry Valleys glacial records show that regional glaciers became cold-based.

Downcutting eventually isolated the Friis Hills plateau, resulting in the preservation of the drift sequence. This event was most likely associated with growth of the East Antarctic Ice Sheet 14 Ma ago. This age constraint means that the tills preserved in the Friis Hills date from a time just before the East Antarctic Ice Sheet expanded and became a permanent feature. Based on the age-dated stratigraphy presented in this thesis, future work focusing on fossiliferious interbeds could provide unique and important constraints on Miocene climate change.

ACKNOWLEDGEMENTS

I need to acknowledge many people for assisting my graduate school endeavors. Most importantly, I would like to thank my ever-patient advisor, Dr. Adam Lewis. He provided me with the necessary tools to become a successful student and writer. I would like to thank him for giving me financial support and academic guidance over the past two years. I am also deeply indebted to the Environmental and Conservation Science program and the Department of Geosciences at North Dakota State University for additional financial support. Next, I would like to thank my committee members Dr. Allan Ashworth, Dr. Bernhardt Saini-Eidukat, and Dr. Thomas DeSutter for their guidance throughout this process. Also Chad Crotty, Michael Ginsbach, Marianne Okal, Spencer Salmon, and Felix Zamora for assistance with fieldwork and laboratory work. Without them, I would not have been able to complete such a large venture. I would also like to thank my parents for teaching me the importance of good work ethic. Lastly I thank my wife Lisa. I could have not accomplished any of this without your loving support.

TABLE OF CONTENTS

LIST OF TABLES

LIST OF FIGURES

LIST OF FIGURES (continued)

LIST OF APPENDIX TABLES

LIST OF APPENDIX FIGURES

CHAPTER 1. INTRODUCTION

Beginning in the early Eocene, approximately 50 million years ago (Ma), global climate began a long-term cooling trend (Zachos et al., 2008) (Figure 1.1). The cooling was punctuated by three large steps, the first in the earliest Oligocene (34 Ma), the second in the middle Miocene (14 Ma), and the last in the mid-Pliocene boundary (3 Ma) (Zachos et al., 2001a, 2008). The first cooling step was associated with the initial growth of Antarctic ice sheets and the initiation of the Antarctic circumpolar current (ACC), whereas the last was associated with the closure of the Panamanian oceanic gateway and growth of ice in the northern hemisphere (DeConto and Pollard, 2003; Ruddiman and Raymo, 1988). In contrast, the cooling episode in the middle Miocene has no clear cause. It has been called the Mid-Miocene Climate Transition (MMCT) and appears to involve a reorganization of the Earth's ocean-atmosphere system (Miller et al., 1987; Shevenell et al., 2004, 2008),

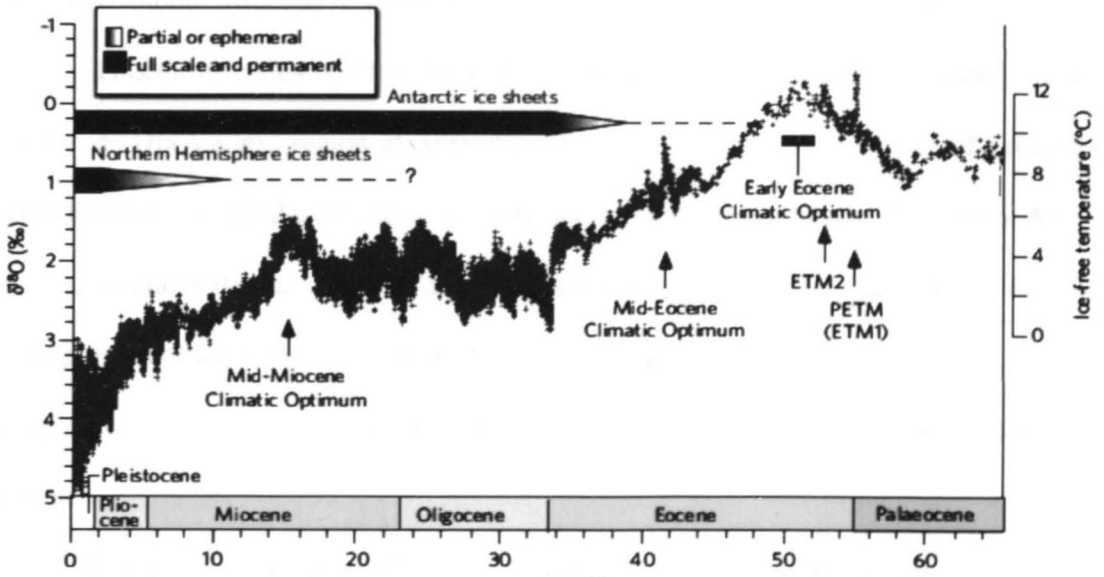

Figure 1.1. Zachos et. al., 2008, global-ocean $\delta^{18}O$ curve showing the cooling of global climate over the past 50 Ma. The MMCT is the steep cooling and ice-growth event at 14 Ma. It occurs just after the Mid-Miocene Climatic Optimum (identified in the figure) at 17 to 15 Ma.

following a 10-Ma-long period in the early Miocene of stable or even slightly warming climate (Zachos et al., 2008; Naish et al., 2001).

Antarctic paleoclimate information for this important period of climate change is generally lacking. Changes in ocean circulation, temperature and chemistry during the MMCT make marine records difficult to interpret and, in some marine basins, caused dissolution of the carbonate record (Shevenell et al., 2008). For Antarctica, glacial-marine records of this age are preserved in just a few tectonic basins (Naish et al., 2009). Most were eroded away when ice sheets expanded to the continental shelves during middle- and late-Miocene time (Bartek et al., 1991; Bart et al., 2000). The terrestrial record of the MMCT in Antarctica comes from just one region in the western Olympus Range where an exceptional glacial record registers a change in glacial thermal regime and the extinction of a terrestrial biota at 14 Ma (Lewis et al., 2007, 2008). More information is needed from the early and middle Miocene to understand Antarctica's role in the MMCT.

This thesis centers on the study of a suite of tills in the Friis Hills, located in the McMurdo Dry Valleys region of Antarctica (Figure 1.2). These tills are part of a record of late-Oligocene to middle-Miocene age glaciation in the Transantarctic Mountains. At several locations they are interbedded with paleosols and lacustrine deposits that developed during times of ice recession. Together the tills and fossil-rich interbeds register temperature and ice conditions for a critical time in the evolution of the global climate system.

The outcrop pattern of tills in the Friis Hills complicates their study. Along the eastern edge of the Friis Hills a sequence of stacked tills fills a shallow paleovalley, which is cut into underlying granite bedrock. This till sequence includes a dated volcanic ash

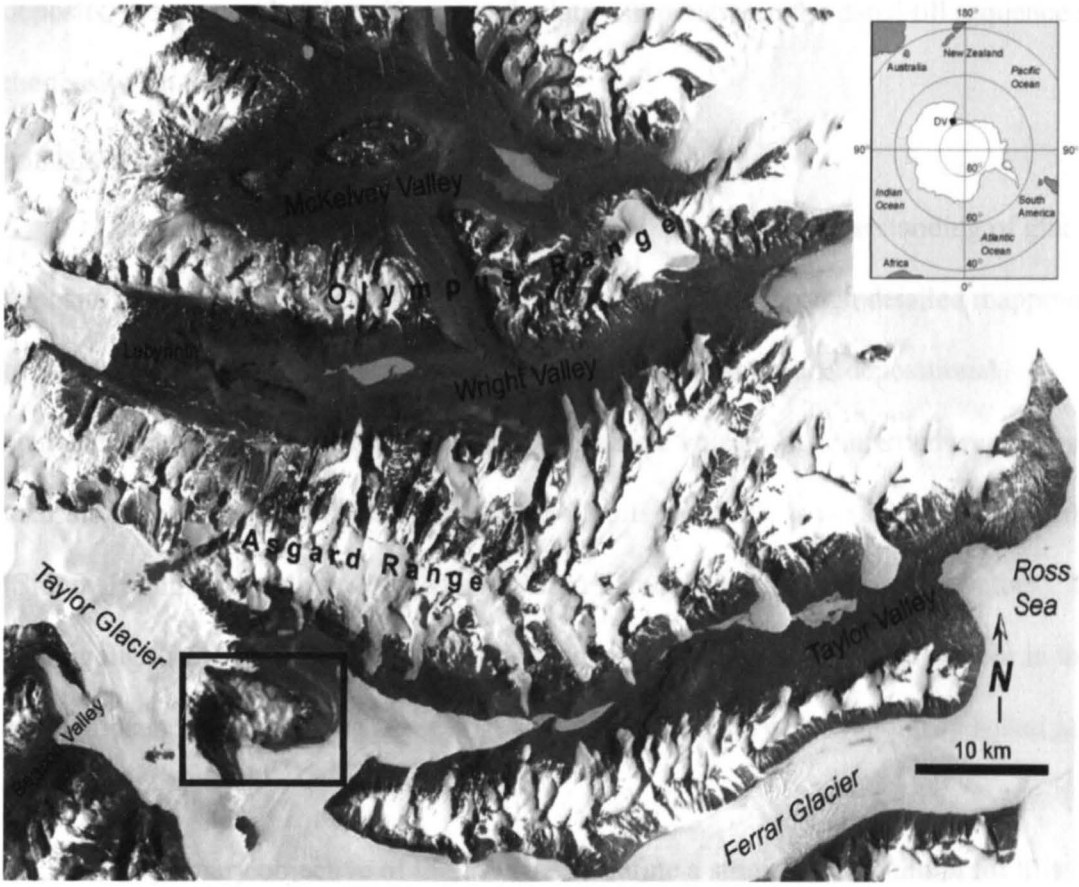

Figure 1.2. Satellite image of the McMurdo Dry Valleys. The Friis Hills plateau is located in the black box; clouds partially obscure the central portion of the plateau. Ice from the East Antarctic Ice Sheet flows from Taylor Dome (approximately 80 km west of the Dry Valleys) towards the Ross Sea coast (right margin of the image). This ice nourishes Taylor Glacier, which flows around the Friis Hills before it terminates on the floor of Taylor Valley. NASA satellite image.

interbed that provides a firm limiting age for the sequence. Two km to the west, near the center of the Friis Hills plateau, a sequence of stacked tills fills a small topographic depression. This till sequence includes several laterally extensive fossil-rich interbeds that have been used to provide estimates of terrestrial climate conditions (Ashworth et al., 2011). An expanse of barren bedrock separates these two till sequences making direct correlation impossible. Before a complete climate record can come from the study of these

deposits, the temporal and environmental relationship between the dated till sequence and the fossil-rich till sequence must be known.

Goals and Objectives of the Thesis

The main goal of this thesis is to build a comprehensive understanding of glacial deposits in the eastern Friis Hills. This will be accomplished through detailed mapping of till sheets and an analysis of internal stratigraphic relationships and depositional characteristics. Earlier fieldwork showed that a single volcanic ash interbed was exposed near the base of the till sequence. Laboratory results showed that the ash was 19.76 Ma old (Sidney Hemming, preliminary lab report from Lamont-Doherty Earth Observatory). The age highlights the importance of the tills for paleoclimate research. It places them in the early Miocene when the long trend of global climate cooling was temporarily halted just before the MMCT.

The primary objective of this study is to define a stratigraphic column for tills in the eastern Friis Hills, which critically includes the age relationship of the dated volcanic ash to the till sequence. During fieldwork, a new volcanic ash bed was discovered that will provide a second chronologic control point for till stratigraphy. A secondary objective is to use till characteristics to build a glacial history for the Friis Hills. Previous field observations of bedrock striations showed that ice flowed through the Friis Hills from different directions at different times. Likewise, differences in clast lithology suggest changing ice source regions through time. By assigning flow directions to specific tills in the sequence and by quantifying changes in tills, such as clast lithology, the early to middle Miocene evolution of Antarctic glaciers and ice sheets might become better understood.

Lastly, this thesis is a first step toward the possible correlation of tills from the central Friis Hills to those of the eastern Friis Hills. Any future analysis of samples collected from the central Friis Hills outcrops can be compared to this study to make correlations between the fossiliferous tills from the central Friis Hills and the dated tills in the eastern Friis Hills. Although not an objective for this thesis, it is a long-term goal of the research project, which will ultimately provide an age estimate for fossil assemblages.

Friis Hills geologic background

The Friis Hills are located in the McMurdo Dry Valleys sector of the Transantarctic Mountains in southern Victoria Land, Antarctica (Figure 1.2), centered at 77° 45'E, 161° 30'S. The Friis Hills is a plateau detached from the east-west trending mountain ranges that make up much of the Dry Valleys region. The plateau is approximately 8 km long (east-west) by 4 km wide (north-south); the average elevation of the plateau surface is 1,300 m above sea level (Figure 1.3). Late Proterozoic-age granite basement rocks of the Cavendish Pluton are exposed at the plateau surface and along the steep cliffs that bound the Friis Hills plateau to the north, east, and south (Allibone et al, 1993). A 200- to 300-m-thick sill of Ferrar Dolerite, which intruded the granite in the early Jurassic, is exposed along all sides of the Friis Hills plateau (Figure 1.3) (Barrett, 1981). A second Ferrar dolerite sill comprises groups of low hills that stand 50 to 100 m above the plateau surface. Along the eastern margin of the plateau, a 10-m-thick fragment of sandstone bedrock separates Cavandish Granite from the upper sill or Ferrar Dolerite. The sandstone rests on a nonconformity; a 20-cm-thick baked zone marks the contact with overlying dolerite. Over most of the region, the sill followed the nonconformity, but here a small lens-shaped

remnant of sedimentary rock was preserved above the granite along a lateral distance of approximately 200 m.

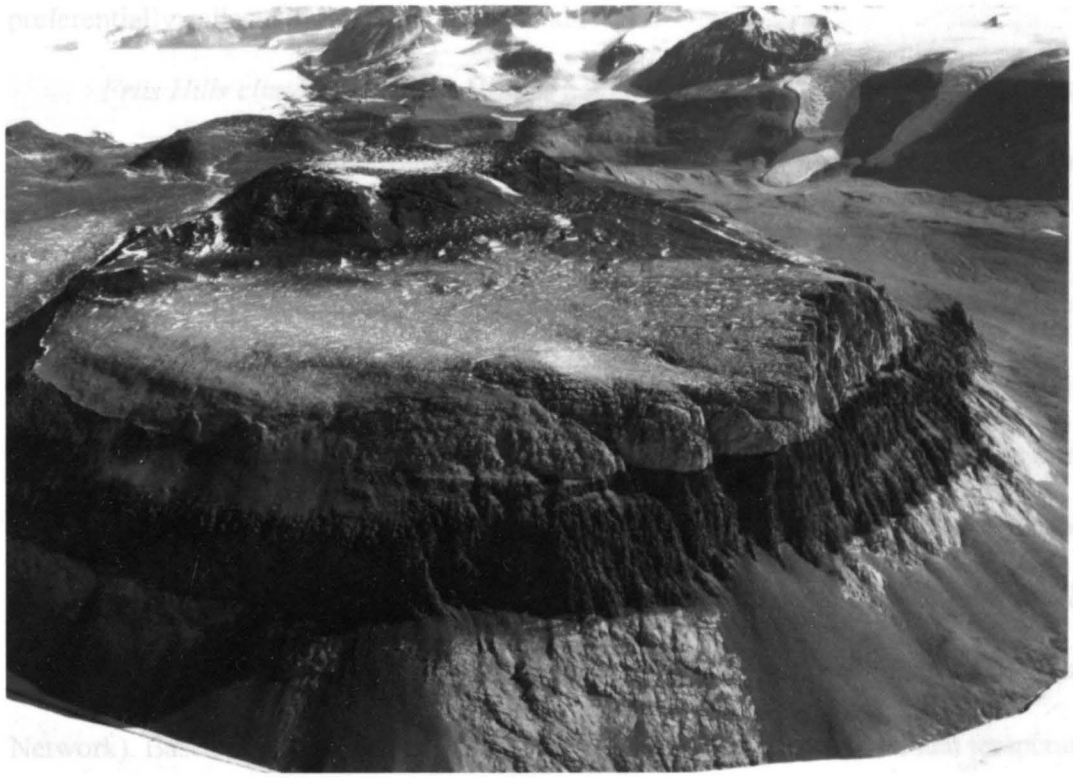

Figure 1.3. Aerial photo of the eastern Friis Hills plateau. Taylor Glacier in the foreground and Pearse Valley in the background to the right; view is to the west-northwest from an elevation of 2000 m. Cavendish Pluton granite is the light colored rock exposed at the plateau surface and in the steep cliffs and slopes above Taylor Glacier. Sills of Ferrar Dolerite form the dark band in the cliff face, approximately 200 m thick, and make up the hills rising above the plateau surface. Light-colored sandstone bedrock is visible near the center of the image as a thin white band below the upper dolerite sill.

Glacial downcutting has transformed the Friis Hills from a more extensive upland to an isolated erosional remnant. Taylor Glacier, one of the main outlet glaciers in the Dry Valleys region, flows around the Friis Hills (Figure 1.2). On the west end of the Friis Hills, the glacier surface is 100 to 200 m below the elevation of the plateau; after being deflected first southward, and then eastward, the glacier surface is 500 m below the plateau (Figures 1.2 and 1.3). Because the Friis Hills redirects Taylor Glacier to the south, the northern slopes of the plateau and adjacent Pearce Valley are ice-free. Very little ice or permanent

snow are present in the Friis Hills. Only small accumulations of ice and snow occur in the low hills that rise above the plateau surface, typically where wind-blown snow preferentially collects in the lee of slopes and ridges.

Friis Hills climate. The Friis Hills is a polar desert with subfreezing temperatures and strong winds occurring throughout the year. Located at the highest elevation in the Friis Hills, a meteorological station recorded weather conditions from 2005 to 2010. During this period mean summer temperature was -13.2° C, with an average wind speed of 4.7 m/s; the winter mean was -29.7° C, with an average winds speed of 4.2 m/s (Bliss et al., 2011). The best estimate for long-term climate conditions in the Friis Hills comes from Lake Bonney, 10 km to the east, where meteorological data have been recorded for the last two decades. Mean annual temperature at Lake Bonney for the years 1986-2000 and 2005-2010 is -17.9° C (Doran et al., 2002; 2005-2010 data from Long Term Ecological Research Network). Based on a dry adiabatic lapse rate of 9.8° C/km, the mean annual temperature in the Friis Hills is estimated to be -30.1° C. Maximum summer temperatures at Lake Bonney typically remain just below freezing (Doran et al., 2002). Using the dry lapse rate this equates to maximum summer temperatures in the Friis Hills of -13 to -14° C (Table 1.1). Average wind speed for Lake Bonney is 3.9 m/s, with a max recorded speed of 35.6 m/s (Doran et al., 2002). The Friis Hills likely experiences stronger average winds because of the high elevation and surrounding smooth glacial surfaces.

Table 1.1. Mean monthly temperature averaged for years for 2005-2010 for the Friis Hills in degrees centigrade. Temperature is extrapolated from Lake Bonney, based on the dry lapse rate of 9.8° C/km. Data from the Long Term Ecological Research Network (http://tropical.lternet.edu:8080/knb/metacat?action=read&qformat=lter&insertTemplate=0&docid=knb-lter-mcm.7003.5, 1st August, 2011).

Jan	Feb	Mar	Apr	May	June	July	Aug	Sept	Oct	Nov	Dec
-13.64	-21.44	-32.17	-37.50	-37.15	-38.25	-41.68	-40.08	-36.17	-30.31	-19.15	-13.88

CHAPTER 2. METHODOLOGY

Field Methods

Fieldwork in the eastern Friis Hills was conducted from October to December, 2010. Objectives of the field study included examination of tills exposed in hand-dug excavations, collection of sediment samples for later laboratory analyses, and the mapping of identifiable till units exposed at the surface using GPS.

Excavations and field descriptions. I exposed glacial sediments in 72 hand-dug pits in the eastern Friis Hills. Pits were excavated to expose specific beds of till, particularly thick stratigraphic sequences, or contacts between tills. Pits were kept to a minimum size in order to reduce environmental impacts but were expanded where needed to expose stratigraphic contacts. Pits were typically less than one cubic meter in size but some were as much as 7 m long and 1.2 m deep. For each pit I recorded the GPS location and characteristics of local topography. Digital images were taken as a record of till appearance with special emphasis on stratigraphic contacts and vertical pit surfaces. Sedimentological characteristics noted in the field included grain size, clast lithology, clast texture, color, and longitudinal axis of buried clasts, as well as any transitions in these characteristics in pit stratigraphy.

Representative till samples were collected from each stratigraphic unit exposed in excavations. All samples were sieved in the field through a 16 mm (-4 ϕ) screen to separate cobbles and boulders from gravel and matrix. Clasts larger than 16 mm (-4 ϕ) were counted and placed in labeled canvas bags. A minimum of 40 clasts were collected for each sample location. Matrix samples, collected in a pan below the sieve, were placed in labeled Whirl-pack plastic bags. Volcanic ash samples were collected separately using a clean

spoon or spade to avoid potential contamination. Ash was placed in labeled bags and stored separately from sediment samples. Once sampling was completed, each excavation was refilled.

Characterization of surficial geology. Most of the tills preserved in the eastern Friis Hills outcrop on east- and west-facing slopes in erosional truncations (Figure 2.1). Viewed from above, tills appear as stacked, lens-shaped beds identifiable on the slope by changes in color and texture. To help differentiate tills at the ground surface, boulder counts and clast lithologies were logged along down-slope transects. To do this I walked transects from the highest point on the truncated section, typically the ridge top, directly downslope to the point where underlying bedrock is exposed. Each transect was created using a 100-m-long measuring tape with the start and finish point of each transect being recorded using GPS. Eight transects were walked, spaced 100 m apart; they ranged in length from 35 m to 138 m. Each transect was oriented as near as possible to perpendicular to the ridge and contacts. I recorded boulders larger than 30 cm that fell within 1 m on either side of the tape. The number of boulders counted in each transect ranged from 17 to 109.

GPS and GIS mapping. GPS coordinates were recorded for all 72 excavations sites and 8 surface-boulder transects using a Trimble Pro XRS. Contacts between sedimentary units observable at the ground surface were recorded with Trimble 5700 Post-Processing Kinematic (PPK) survey equipment and then were converted for ArcGIS in Trimble Geomatics Office (TGO). This was accomplished by walking along contacts while the Trimble unit recorded a point location every 5 seconds. Each contact walked in the field was given a unique file name, which was later converted to a map line in ArcGIS. These lines were compiled to form a geological surface map. Maps resulting from this GPS

Figure 2.1. Northeast-facing slope in the eastern Friis Hills. The image is from a point approximately 800 m above the surface of Taylor Glacier, 1 km east of the plateau edge. This slope exposes the bedrock-floored paleovalley and displays the stacked tills filling the valley in a sharp erosional truncation. Surface boulder counts took place on this slope; only two excavations were made on the slope because ice-cemented permafrost occurs only 10 to 15 cm below the ground surface

survey are presented in section three; results from boulder counts are compiled in Table 3.2.

Laboratory Methods

All laboratory analyses follow the procedures of Folk (1974). Analyses were conducted at NDSU in the Department of Geosciences.

Clast Analysis. Clasts larger than 16 mm (-4 ϕ), were scrubbed and rinsed in tap water in order to remove adhering sand and silt-sized particles. Once dry, each clast was

examined on the basis of lithology, striations, molding, desert varnish, staining, and ventifaction. A total of 1,128 clasts were examined.

Sediment Analysis. Gravel between 2- to 8-mm diameter (-1 ϕ and -3 ϕ) was sieved at four different intervals using standard dry sieve techniques and an automated Ro-tap shaker. Weights of sediment retained at each interval were recorded to the nearest 0.01 g using an Ohaus Adventure Pro scale. The weighed gravel samples were then placed in a plastic bag and labeled for future use.

Sand analysis was completed by first collecting a 70 to 100 g split from the material that passed through the gravel-size sieves. Sample splits were washed with deionized water (DI) to remove salt. All splits were washed at least 3 times, each being allowed to soak and settle undisturbed for at least 24 hours. This allowed for the sand and mud to settle. The wash water was then carefully decanted from each beaker so that even silt and clay-sized sediment was retained. Salt-free samples were then washed with a 2.5g/L Calgon solution through 0.031 mm (5 ϕ) sieve, which collected sand but allowed mud to drain to a 1 L Nalgene bottle. Once dried, the sand was sieved, weighed at intervals from 1- to 0.0625-mm (0 ϕ to 4 ϕ), and then stored, using the same procedures described for gravel.

Pipette analysis was used to determine the proportion of silt and clay in the mud fraction. The mud and Calgon solution was transferred from the Nalgene bottle to a 1 L graduated cylinder. When necessary, additional Calgon solution was added to the cylinder to bring the volume of the solution to 1 L. Using a stir rod, the solution was vigorously stirred developing uniform distribution. Once the stir rod was removed, 20 ml subsamples were removed from 10 cm depth at time intervals calculated from Folk (1974). Each 20 ml

subsample was placed in a beaker. Each subsample was dried at 97° C and then weighed to the nearest 0.01grams.

Geochronology. Volcanic ash samples were washed in deionized water to remove salt and clay particles. Each sample was placed in a Branson 3510 sonicator for 20 minutes, which released clay from grain surfaces and from most vesicles. The clay, while still in suspension, was poured off by hand. A small fraction of silt-sized and fine, sand-sized grains were also lost in this process. Dried sample splits were examined using a Lieca M165C binocular microscope at 10 to 65x magnification. Sanidine crystals were identified on the basis of cleavage, color and crystal habit. The largest, ranging from a maximum diameter of about 300 μm to a minimum of about 50 μm, were handpicked and placed in a cleaned, labeled glass vial. This subsample of crystals was sent to Lamont-Doherty Earth Observatory for $^{40}Ar/^{39}Ar$ analysis on 2 May 2011.

Surface clasts were also collected from the Friis Hills for possible future use in exposure-age dating. Exposure samples were taken from identified units based on field mapping. Samples were selected based on size and morphology. Samples that were shielded by nearby upstanding boulders were rejected in favor of unshielded samples. The location of each sample was recorded with GPS and photographed to show local surroundings. Some samples consist of whole surface clasts, the largest of which are 30 cm in diameter. Most samples, however, come from large clasts that were broken into manageable sample sizes. Once a sample was broken, the piece was marked showing which face was originally upward and then photographed again displaying how the sample broke in relation to the original rock shape. Each exposure sample was placed in a labeled canvas bag, which are now stored in the NDSU Geosciences storage facility.

CHAPTER 3. RESULTS

A sequence of till sheets, interbedded with outwash sediments, fills an east-west trending paleovalley in the eastern Friis Hills (Figure 2.1). Field results indicate that a wet-based alpine glacier, flowing to the NE at about 029°, cut the paleovalley into granite bedrock. The glacial and glaciofluvial sediments filling the paleovalley can be separated into two drifts: a stratigraphically lower drift comprised of two tills with thin interbeds of glaciofluvial volcanic ash, sand and gravel, and a stratigraphically higher drift comprised of interbedded ablation tills and proglacial fluvial deposits (Figure 3.1). In this thesis I name the lower drift the Friis drift, based on its location and hypothesized ice source, which is within the Friis Hills. Friis drift can be subdivided into Friis I and II; Friis II being the oldest glacial-geologic map unit in the study area. Based on their association with glacially eroded bedrock surfaces, glaciers depositing these drifts cut the paleovalley through the eastern Friis Hills. In this thesis I have named the upper drift the Cavendish drift, based on its high content of clasts derived from the Cavendish Pluton (Figure 3.2). Cavendish is subdivided into three units called Cavendish I through III. Cavendish I is the youngest glacial-geologic map unit filling the paleovalley study area. Glaciers depositing Cavendish drift flowed obliquely to the paleovalley axis and partially eroded the older Friis drift as well as truncating the paleovalley itself (Figure 2.1).

Friis Hills Morphology

The Paleovalley. Based on an analysis in ArcGIS, the paleovalley is 35 m deep measured from the granite bedrock underlying Friis II to the highest glacially molded bedrock surface. Its axis trends southwest to northeast at an orientation of approximately

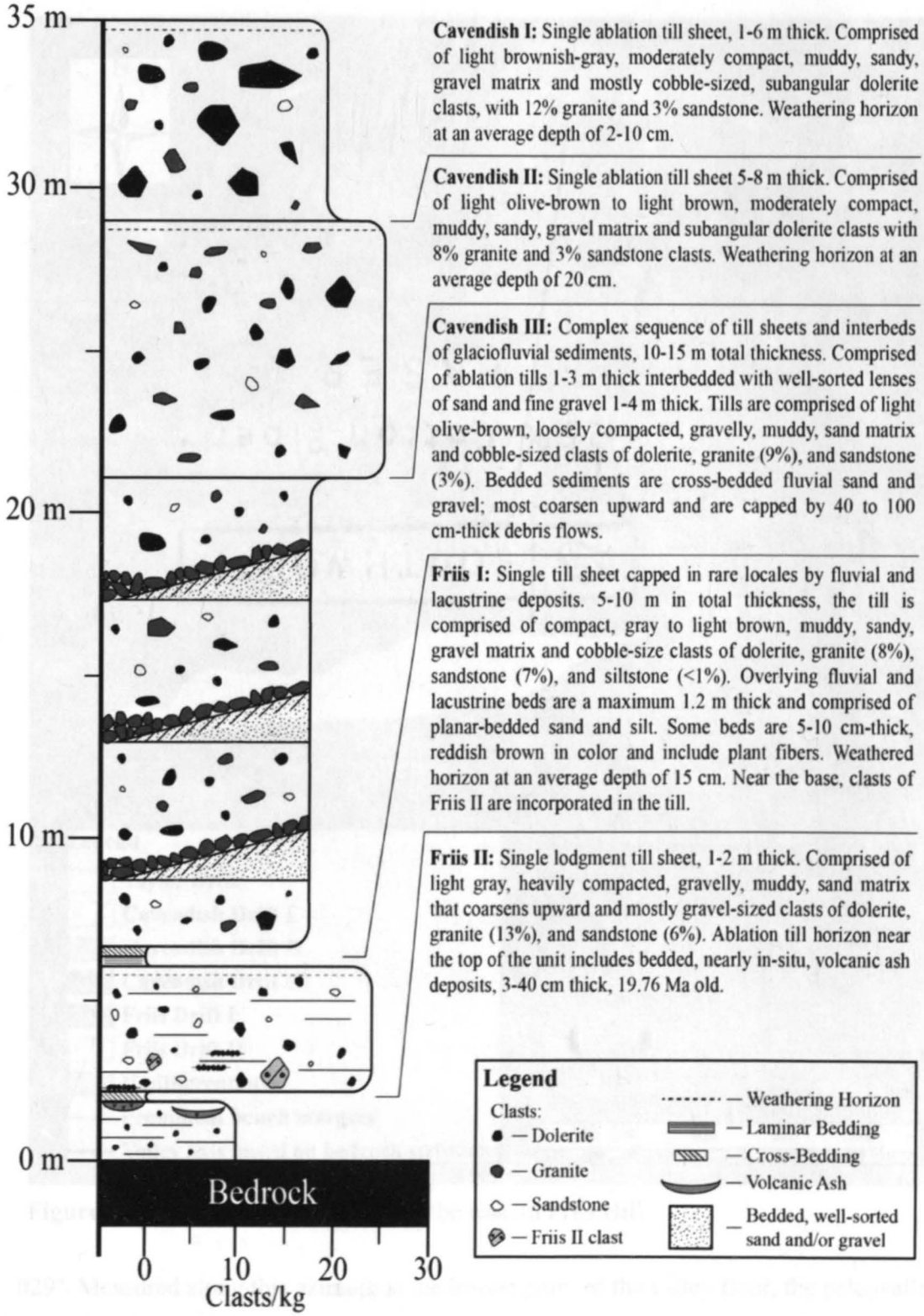

Figure 3.1. Stratigraphic column for glacial deposits in the eastern Friis Hills paleovalley.

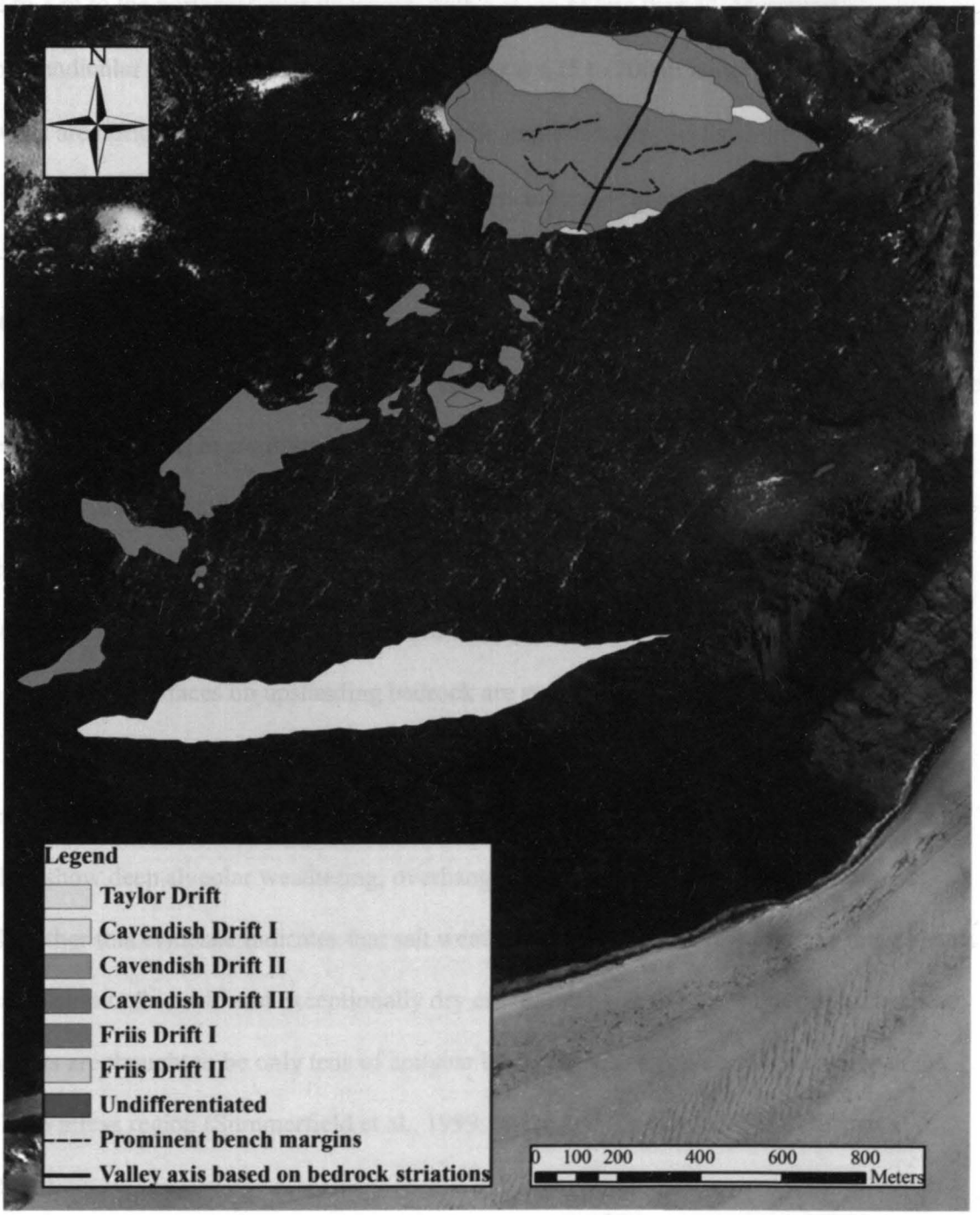

Figure 3.2. GIS map of glacial tills of the eastern Friis Hill.

029°. Measured along this azimuth at the lowest point of the valley floor, the paleovalley extends 570 m. Based on GPS measurements of elevation at each end of the valley, it dips

2 to 3 m to the northeast over its length, with a slope of less than 1°. Measured perpendicular to the valley axis, the paleovalley is 675 to 700 m wide. Although the valley walls are buried, valley width relative to depth suggests valley walls slope at about 6°.

Modern Morphology. At scales of meters to tens of meters, surfaces in the Friis Hills show evidence for slow weathering under an arid climate. In dolerite bedrock, upstanding tors as much as 5 m in height rise above and surround shallow, grus-covered lows. Where granite bedrock is exposed, broad grus-covered plains characterize most of the eastern Friis Hills. In some areas grus as much as 40 cm deep blankets granite bedrock. Near the plateau margins cavernously weathered joint surfaces in the bedrock produce a complex topography of overhanging ledges, from 1 to 3 m high, and elongated tors and yardangs 2 to 4 m in height by 10 to 20 m in length.

Most surfaces on upstanding bedrock are stained only on northeast-facing sides. Likewise, desert varnish and weathering rinds only occur on northeast-facing surfaces. In contrast southwest-facing surfaces appear fresh. Where rock surfaces are convex or where they show deep alveolar weathering, overhanging surfaces are typically salt encrusted. Together this evidence indicates that salt weathering and wind abrasion are the main agents of erosion in this cold and exceptionally dry environment. Rates of weathering from these agents are thought to be only tens of cm/year based on cosmogenic nuclide studies in the Dry Valleys region (Summerfield et al., 1999; Balco and Shuster, 2009; Morgan et al., 2010).

Viewed at scales of hundreds of meters to kilometers, the eastern Friis Hills shows well-developed evidence for glacial erosion. South of the dolerite-capped hills that bound

the study area to the north, the plateau surface has been molded into a series of parallel troughs and ridges oriented roughly east to west.

The most prominent of these is a ridge that extends 1.8 km from a small dolerite-capped knoll, standing about 110 m above the plateau surface, to the southeastern edge of the plateau (Figure 1.3). This ridge is about 300 m wide by 35 m high. Together these features form a classic, glacially carved crag and tail. In this interpretation the dolerite knoll forms a resistant crag that protects a tail of granite extending in the direction of ice flow, approximately 084°. A second crag-and-tail feature, parallel to the first, is situated to the north. The dolerite hills that bound the study area form the crag, whereas the tail holds the paleovalley and drift sheets. The tail extends to the east for a short distance before being truncated by the plateau edge. The north-facing slope of the tail is angled at 9°; the south-facing slope is angled at 7°.

Situated between these two crag-and-tail features, and running parallel to them, is a shallow glacial trough which bisects the plateau surface in the eastern Friis Hills. The trough originates from a low, dolerite-floored saddle between the two crags described above and extends about 2.1 km to the east (Figure 1.3). It is only a few meters deep adjacent to the crags but reaches a depth of about 35 m where it is truncated at the southeastern plateau margin. The trough's orientation is 086° measured from satellite imagery. The northern slope of this trough crosscuts the paleovalley and the till sheets that fill it. This slope and associated truncation surface are orientated at 083°. The paleovalley floor, both valley walls, and drift sheets that fill the valley, are exposed on this slope.

The crag-and-tail features, bedrock trough and the erosional truncation of the more ancient paleovalley all provide evidence that glacial erosion has shaped and streamlined the

eastern Friis Hills. Although subaerial processes are continuously altering this topography to the point that it is obscured at scales of tens of meters, evidence for glacial erosion remains.

Glacial deposits in the eastern Friis Hills – overview

Glacial deposits in the eastern Friis Hills are separated into two groups based on differences that are evident in the field as well as in laboratory analyses. From field observations, tills comprising Friis drift are thin and show simple, subdued, low-relief surfaces (Figure 3.3). Tills and interbedded sediments in Cavendish drift are thick with complex internal bedding, which results in high-relief surfaces of stepped benches and steep erosional margins (Figure 3.3). Differing surface color comes from lithology and weathering characteristics. Boulders and cobbles exposed at the surface of Friis drift are

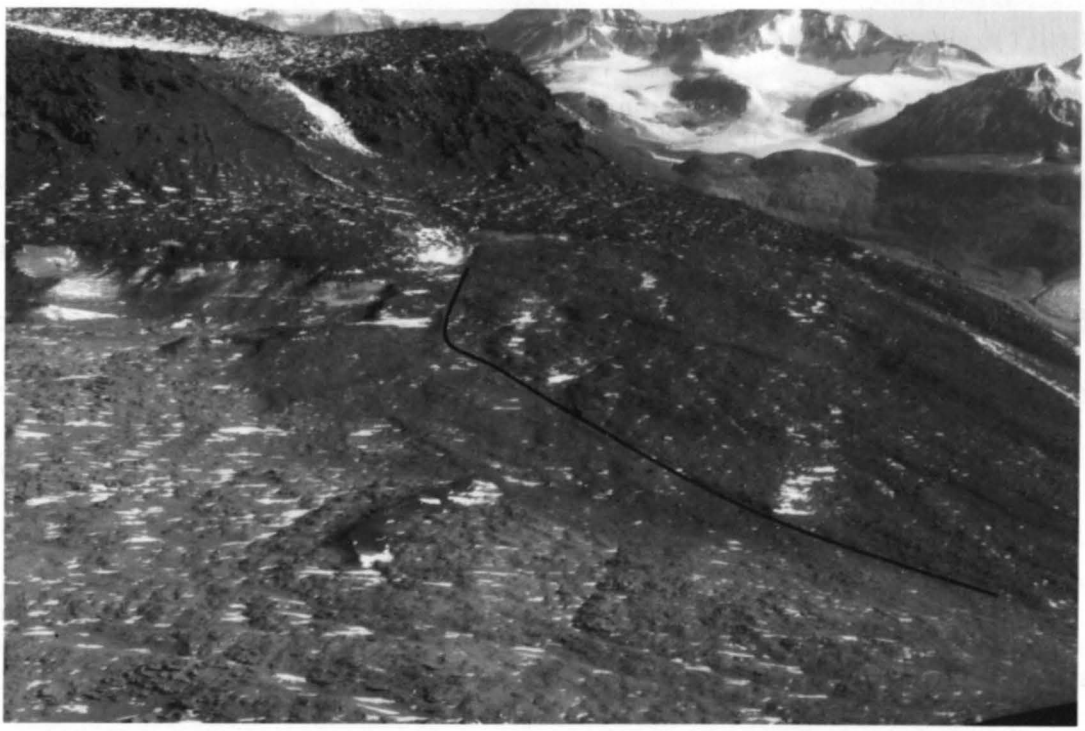

Figure 3.3. Aerial photo of Friis and Cavendish drifts. Line separates the gently sloped Friis drift to the left and high-relief, erosional ridged Cavendish drift to the right.

mainly dolerite and most are deeply weathered, which produces a deep red to nearly black surface coloration. In contrast, surfaces of Cavendish drift are made up of granite, dolerite and sandstone boulders, which weather to red to reddish-brown colors.

Lab analysis also shows differences in characteristics between the two drifts. Tills in Cavendish drift all show similar percentages of gravel, sand, and mud, whereas tills in Friis drift have lower percentages of gravel and correspondingly higher percentages of sand and mud. In Friis drift sandstone clasts are more abundant than in Cavendish drift. Granite clasts derived from local bedrock are generally more common in Cavendish drift although the unit resting on bedrock, Friis II, has the highest percentage of granite clasts. This results from a few samples skewing the average due to a large numbers of bedrock fragments. Lastly, clasts in Cavendish drift are more commonly molded and polished than are those from Friis drift.

In the following sections, analytical results for all five subdivided units of Friis and Cavendish drifts are given in stratigraphic order from top to bottom. Outcrop patterns, results from GPS-assisted field mapping, and surficial morphology are given first. Textural analyses of till matrix and results of clast analyses follow. Lastly evidence for ice flow directions is given. All laboratory results are summarized in tables within this chapter; full results are given in Appendix A and B. Surface boulder counts are presented in Appendix C.

Cavendish I

Characteristics. Cavendish I is a 1- to 6-m-thick, partially lithified, light brownish-gray (2.5Y 6/2), cobble-rich diamicton. It has a surface area of approximately 2,900 m^2

(Fig 3.4). In map view it crops out in an elliptical shape approximately 100 m long by 39 m wide with the long axis oriented roughly north-south. It is the highest stratigraphic unit in the study area and caps the sedimentary sequence filling the paleovalley (Figure 3.1). To the north Cavendish I rests on Cavendish II; to the south it directly overlies Cavendish III.

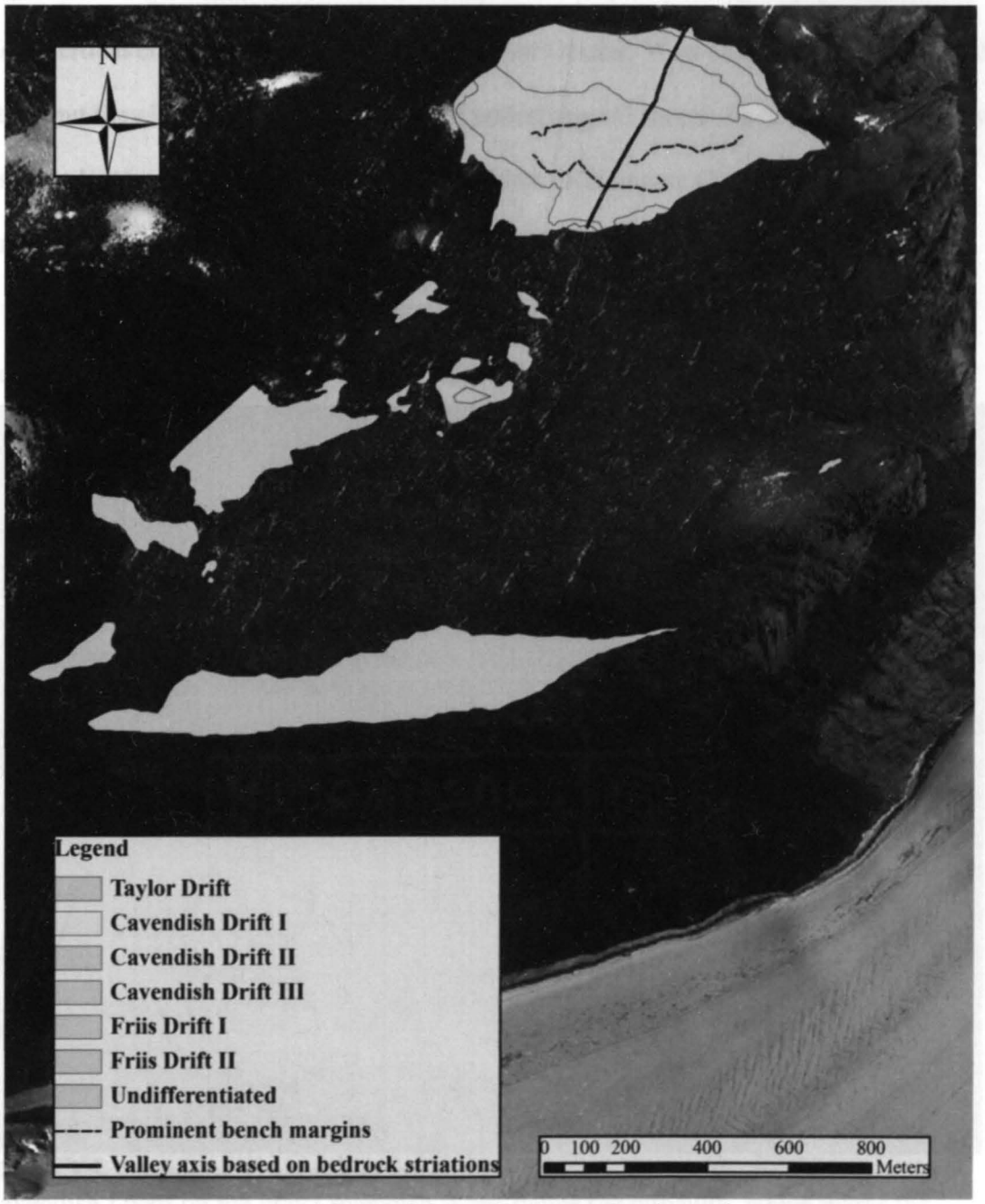

Figure 3.4. Outcrop map of Cavendish I. All other units shown in gray.

Although it was not observed, it follows that the base of Cavendish I crosscuts the contact between Cavendish II and III.

The upper surface of Cavendish I is relatively horizontal. Steep slopes, 3 to 5 m high, mark the margins of the outcrop on all sides. Steep east-facing slopes lead down to a near-vertical cliff that borders the modern Taylor Glacier. West-facing slopes are similarly steep but they lead down to the surfaces of underlying till sheets. These sharp edges as well as abundant, red-stained dolerite surface boulders differentiate Cavendish I from underlying Cavendish II and III at the ground surface.

Based on excavations and sedimentology of surface exposures, Cavendish I is comprised of a single till sheet (Figure 3.5). This till is a compact diamicton made up of

Figure 3.5. Cavendish I exposed in excavation. The light brownish-gray till of Cavendish I rests on the gray Cavendish II and below the tarpaulin, which marks the ground surface before the pit was excavated.

primarily cobble-sized clasts set within a light brown-gray (2.5Y 6/2), muddy sandy gravel matrix (Table 3.1, Figure 3.6). Clasts in the till are dolerite, granite and sandstone. Of these, none are erratics relative to bedrock exposed in the Friis Hills. A third of the clasts are glacially molded, however none shows surface striations (Table 3.2). Surface boulders are mostly dolerite set among a few scattered boulders of granite and very rare sandstone. Some excavations reveal a near-surface weathering horizon that extends to an average depth of 10 cm. A sharp transition from the weathered horizon to the till is marked by a change in color from dark red to light red. Weathering processes have planed some dolerite and granite clasts so that they are level with the ground surface; most of these are surrounded by a thin layer of grus that extends several meters to the northeast, which is the prevailing wind direction (Doran et al., 2002). Cavendish I does not rest on bedrock anywhere in the study area.

Table 3.1. Sedimentological analysis for drifts in the eastern Friis Hills.

	Sedimentology				
	Texture (matrix <1.6 cm)			Mud composition	
Unit	Gvl (%)	Sand (%)	Mud (%)	Slt (%)	Cl (%)
Cavendish I *n*=2	35.3	47.3	17.4	16.6	0.8
Cavendish II *n*=6	32.5	54.8	12.7	11.4	1.3
Cavendish II *n*=13	28.6	53.0	18.4	14.9*	1.6*
Friis I *n*=11	35.6	50.4	14.1	11.0*	1.1*
Friis II *n*=10	23.7	55.5	20.8	24.1*	2.8*

Abberviations:n-number of samples analyzed per till unit; Gvl=gravel; Sand=sand; Mud=mud; Slt=silt; Cl=clay.

*Average values of silt and clay for Cavendish III excludes 3 samples, Friis I excludes 2 samples, and Friis II excludes 7 samples, because of excluded data sums do not equal 100%. Table excludes undifferentiated samples: ASS-10-43A/B, ASS-10-64, ASS-10-74A/B.

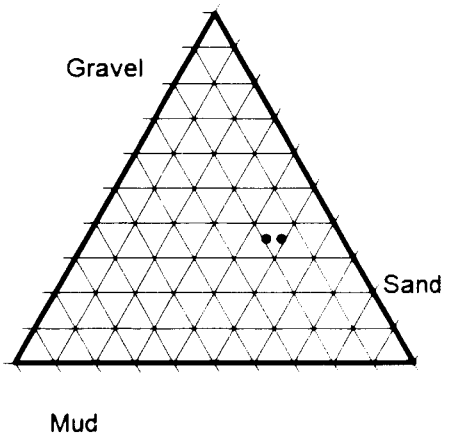

Figure 3.6. Ternary plot of Cavendish I matrix. Based on Folk (1974), the average of the matrix analyzed plotted as muddy sandy gravel. Scales go from 0 to 100%. 100% rests at labeled point; 0% rests at line opposite point.

Interpretation. Cavendish I is the youngest till in the paleovalley. It is a single sheet of ablation till, most likely deposited at the glacier bed. It was deposited by ice that flowed over both Cavendish II and Cavendish III. The fact that Cavendish II is missing beneath the southern outcrop of the till could mean that the ice was erosive in some places. The mud-rich matrix and glacial surfaces on clasts indicate that the ice was wet- based. The ice was locally derived based on the lack of erratic clasts in the till.

Given the truncated edges of the till sheet and its restricted map pattern, Cavendish I has been eroded. Its restricted extent and sharp edges are suggestive of glacial erosion. However, modern subaerial processes such as wind deflation and salt weathering are most likely slowly eroding these slopes at present given evidence for erosion of boulders at the ground surface.

Cavendish II

Characteristics. Cavendish II is a 5- to 8-m—thick, compact, light colored diamicton. It is exposed over an area of 78,400 m^2 (Figure 3.7). Where Cavendish I is

Table 3.2. Clast characteristics for the eastern Friis Hills drift sheets.

	Clasts									
			Glacial Surfaces			Lithology				
Unit	Clasts/kg of matrix (>1.6 cm)	Number of clasts analyzed	Mol (%)	Str (%)	Pol (%)	Dol (%)	Gr (%)	SS (%)	Sltst (%)	Errat. Gr (%)*
Cavendish I *n* 2	19	93	30.1	0.0	1.1	84.9	11.8	3.2	0.0	0.0
Cavendish II *n* 6	25	251	35.9	1.6	7.2	89.2	7.6	3.2	0.0	0.0
Cavendish II *n* 13	17	533	22.0	2.1	3.8	86.3	9.6	3.4	0.8	0.2
Friis I *n* 11	20	442	21.9	1.4	1.6	87.1	6.6	6.1	0.2	0.5
Friis II *n* 10	14	435	23.7	0.2	2.1	76.3	17.7	5.7	0.2	0.9

Abberviations:n-number of samples analyzed per till unit; Mol=molded; Str=striated; Pol=polished; Dol=dolerite; Gr=granite; SS=sandstone; Sltst=siltstone; Errat. Gr=erratic granite.

*Erratic granite clasts are those from plutons other than Cavendish.

Table excludes undifferentiated samples: ASS-10-43A/B, ASS-10-64, ASS-10-74A/B.

absent, Cavendish II crops out at the top of the valley fill. Steep erosional edges to the east and west give the till outcrop a ridge-like appearance. In map view it forms a long, narrow ellipse oriented north-south. West-facing slopes are from 4 to 5 m high; east-facing slopes, which are exposed along a steep erosional truncation, are from 5 to 8 m high. Over most of the study area Cavendish II is the highest stratigraphic unit; it underlies Cavendish I only along the southern edge of the paleovalley. Cavendish II rests directly on Cavendish III to the south; to the north it rests on dolerite bedrock of the south facing paleovalley wall.

Based on excavations and internal stratigraphy exposed along erosional truncations, Cavendish II is comprised of a single till sheet. The till sheet is a moderately compact, light brownish-gray (2.5Y 6/2) to light olive-brown (2.5Y 5/3) colored diamicton (Figure 3.8). It is composed of dolerite, granite, and sandstone clasts set within a muddy sandy gravel matrix (Figure 3.9). Clasts range from boulders to cobbles but most are cobbles from 8 to 10 cm in diameter.

Approximately 45% of clasts in the till show glacial surface textures. The till includes no erratic clasts (Table 3.2). Some excavations reveal a near-surface weathering horizon that extends to an average depth of 20 cm. The horizon is marked by a well-defined change in matrix color from brown or reddish-brown near the ground surface to yellowish-brown at depth. The change in color is sharp, occurring over a vertical distance of less than 4 cm. Surface boulders exposed in Cavendish II are dolerite, granite, and sandstone.

Like Cavendish I, clasts at or near the ground surface in Cavendish II are deeply weathered. Weathering processes have planed some dolerite and granite boulders level with the ground surface. Most of these are surrounded by a thin layer of grus that extends from 1

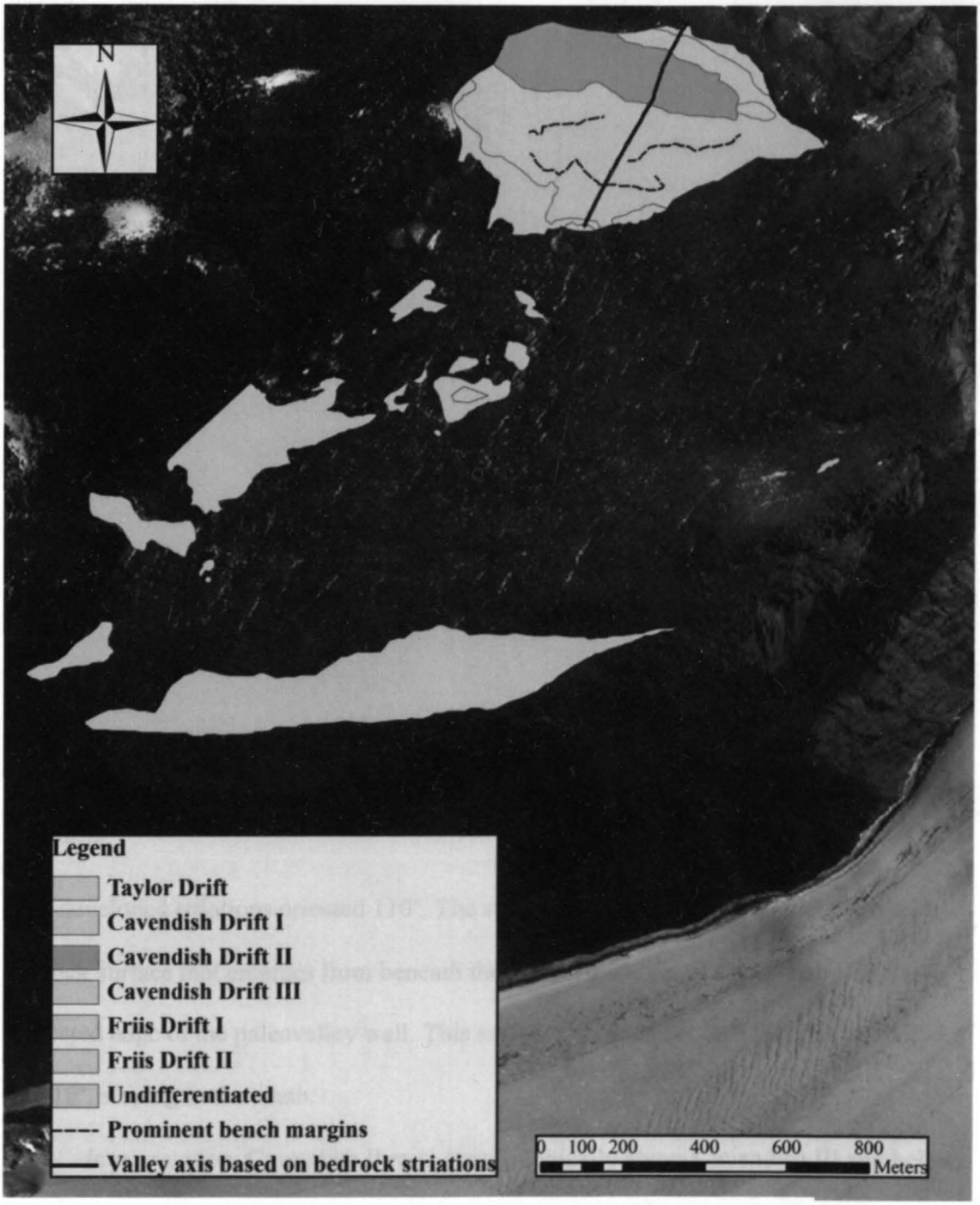

Figure 3.7. Outcrop map of Cavendish II. All other units shown in gray.

to 4 m to the northeast of boulders.

Evidence for ice flow directions comes from a single bedrock exposure that shows

Figure 3.8. Cavendish II exposed near the center of the till outcrop. A brownish weathering horizon transitions to a light brown slightly consolidated matrix at a depth of 20 cm.

well-developed striations oriented 110°. The striations are exposed on a smooth dolerite bedrock surface that emerges from beneath the northern margin of Cavendish II at the truncated edge of the paleovalley wall. This surface descends beneath the till at an angle of 5 to 10°, sloping to the south.

Interpretation. Cavendish II rests stratigraphically above Cavendish III and below Cavendish I (Figure 3.1). It is interpreted as an ablation till deposited at the glacier bed. The fine-grained matrix and abundance of glacially molded and striated clasts indicate that the till was deposited from wet-based ice. Lack of erratic clasts suggests the ice was derived from a local source area. Ice flowed to the east-southeast based on a single striated

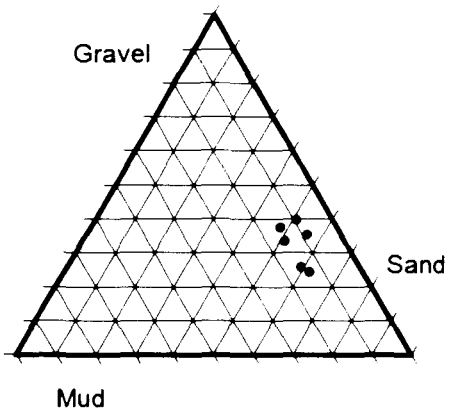

Figure 3.9. Ternary plot of Cavendish II matrix. Based on Folk (1974), the matrices of diamictons in the till sheet are classified as muddy sandy gravel. Scales go from 0 to 100%. 100% rests at labeled point; 0% rests at line opposite point.

surface along the northern margin of the till outcrop. This direction is different from the orientation of the paleovalley, which trends southwest to northeast at about 029°.

The sharp weathering horizon could indicate that the till was exposed at the ground surface for some time prior to burial beneath Cavendish I. However, the horizon was not observed to extend beneath Cavendish I meaning that it could also have developed after deposition of the overlying till sheet. Abrupt truncations on both east and west-facing slopes indicate erosion from glacial activity. Boulders exposed at the ground surface suggest erosion from long-term exposure to subaerial weathering processes in an arid climate similar to that of today.

Cavendish III

Characteristics. Cavendish III is a complex unit comprised of light brownish-gray (2.5 Y 6/2) to light olive-brown (2.5Y 5/3) diamictons interbedded with well-sorted lenses of sand and fine gravel. It is the thickest stratigraphic unit in the study area being 10 to 15 m thick based on GPS mapping of upper and lower contacts. Cavendish III rests above Friis I and below Cavendish I and II (Figure 3.1). In map view Cavendish III extends 55 to

60 m to the east and 315 to 350 m to the west from the map edges of overlying drifts. It covers a map area of 273,500 m^2 (Figure 3.10). To the east, like the two units above it, Cavendish III crops out along a steep erosional truncation overlooking Taylor Glacier. To the west Cavendish III extends from beneath overlying drifts to form a series of nearly level benches. These benches are arranged in stair-step fashion with steep, 3-to 5-m-high, erosional margins separating relatively flat benches. These erosional margins are oriented from 080° to 110°. In cross-section each erosional margin corresponds to a change in internal stratigraphy. Based on excavations into steep erosional margins that exposed internal stratigraphy, Cavendish III is composed of four stacked till sheets. At the base of each till sheet are well-sorted fluvial beds and debris flows deposited in a proglacial setting. The tills are comprised of mostly cobble-sized clasts set within a matrix of gravelly, muddy, sand (Figure 3.11, 3.12; Table 3.1). Based on analysis of 318 clasts, they are primarily dolerite with scattered granite and sandstone; one excavation produced a single siltstone clast (Table 3.2). A low percentage of these clasts are molded compared to those in the other four mapped units. Where tills are exposed at the ground surface, most excavations show a brownish weathering horizon that extends to a depth of 5 to 10 cm.

Below this horizon, tills in Cavendish III have a light olive-brown (2.5Y 5/3) matrix. Interbeds between till sheets are comprised of planar- and cross-bedded sand and gravel (Figure 3.13). Cross-beds dip to the northeast in four excavations. Each interbed is 1 to 4 m thick and has a sharp contact with underlying diamictons. Some interbeds show coarsening-upward sequences of sand grading to gravelly sand, which grades to gravel. Stratified, clast-rich beds cap each sequence above sharp contacts. These capping beds grade upward into unstratified diamictons.

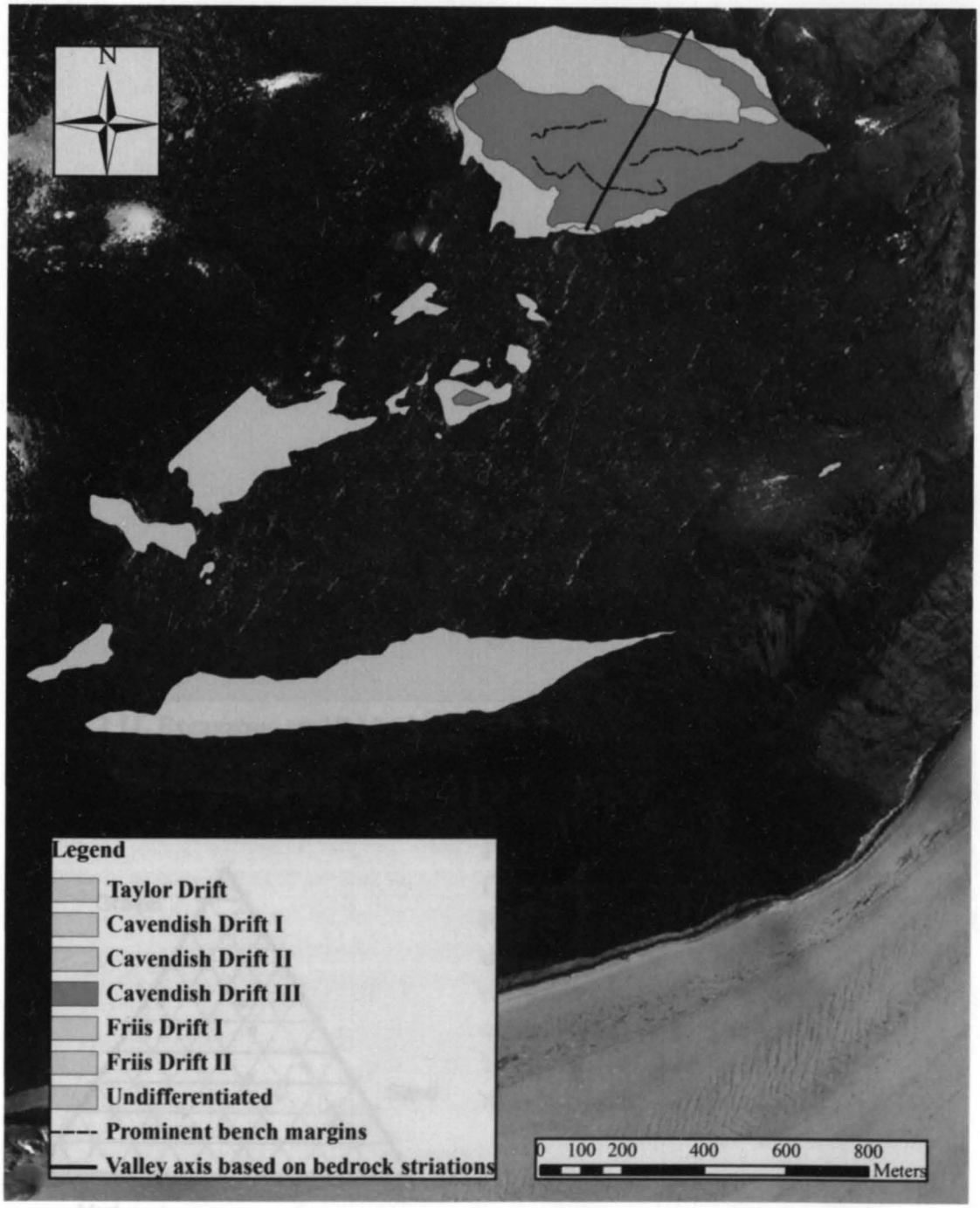

Figure 3.10. Outcrop map of Cavendish III. All other units shown in gray.

The thickness and lateral extent of tills sheets and interbeds appear to control local surface morphology in the unit. Sand and gravel interbeds crop out along the steep margins of benches, whereas diamictons crop out on bench surfaces. Indicators of ice flow direction

Figure 3.11. Excavation pit 10-17 of Cavendish III. Coarse gravel horizon near the surface fines downward. Clasts display molding in the semi-compact till.

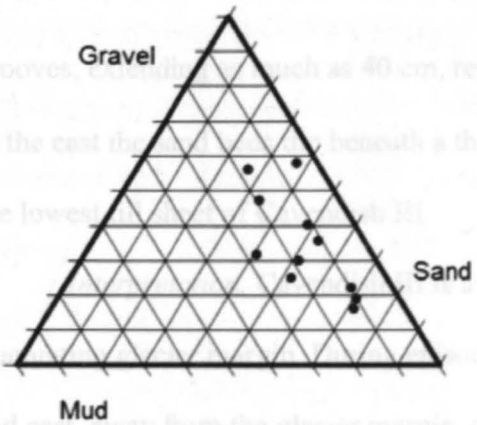

Figure 3.12. Ternary plot of Cavendish III matrix. Based on Folk (1974), the matrices of diamictons in the till sheet are classified as a gravelly muddy sands. Scales go from 0 to 100%. 100% rests at labeled points; 0% rests at line opposite point.

for Cavendish III come from an isolated patch of drift located about 200 m southwest of the main drift outcrop. An excavation into the southern margin of this drift outlier exposed planar-bedded sand resting on polished and striated bedrock. Striations and shallow

Figure 3.13. Excavation pit 10-25 in Cavendish III is located up slope from the erosional benches. This pit displays well-sorted interbeds within the till sheet. These interbeds are comprised of planar and cross-bedded sand and fine to medium gravel. Ground surface to the bottom of the excavation pit is approximately 80 cm.

grooves, extending as much as 40 cm, register flow to the east at 072°. Approximately 4 m to the east the sand beds dip beneath a thin diamicton interpreted in the field to be part of the lowest till sheet of Cavendish III.

Interpretation. Cavendish III is a series of ablation tills deposited beneath a fluctuating glacier margin. During episodes of ice retreat, water flowing to the northeast and east, away from the glacier margin, deposited well-sorted beds of sand and gravel. Coarsening upward sequences suggest most record the advance of glacier ice. Stratified diamictons that cap these beds are interpreted as debris flows cascading from nearby moraines or the ice itself. These indicate a nearby ice margin. Ablation till was deposited

directly from melting ice when the glacier advanced over these sites. Subsequent ice retreat allowed the depositional sequence to be repeated.

Cavendish III rests stratigraphically above Friis I and below Cavendish I and II. Given the mud-rich matrix and glacially molded and striated clasts, glaciers depositing the drift were wet-based. Based on a single striated bedrock surface the ice depositing at least one of the tills sheets was flowing to the east. Whereas overall clast lithology for this till is unremarkable, a single fine-grained, white plagioclase-rich granite erratic was found during clast analyses suggesting this till might have been deposited from ice originating outside of the Friis Hills. The orientations of cross beds, and of wedge-shaped debris flows, suggest that ice margins were retreating and advancing in a northeast-southwest direction. Given the ice flow direction indicated from striations, these margins may have been lateral rather than terminal.

Excavations into benches and their erosional margins show that internal stratigraphy controls drift surface morphology. Tills underlie benches, clast-rich debris flows typically crop out at bench edges, and bedded sand and gravel underlie steep slopes. This suggests that the clast-rich debris flows and ablation till sheets are protecting underlying beds of sand and gravel from erosion. Based on the number of benches displayed at the ground surface, at least four advance and retreat sequences are recorded within this 10- to 15-m thick unit.

The 5- to 10-cm-thick weathered horizon implies subaerial weathering processes. It is not clear from stratigraphy exposed in excavations, however, if this horizon follows the modern surface, meaning it is forming today, or follows the upper surface of the unit, meaning it formed before the deposition of Cavendish II.

Friis I

Characteristics. Friis I is a 5- to 10-m-thick, consolidated, light olive-brown (2.5Y 6/2) to brown (10YR 5/3) colored diamicton. It has a surface area of 153,620 m^2. In map view it crops out as thin bands where it emerges from beneath overlying drifts (Fig 3.14). It also crops out in isolated patches where it mantles slopes leading up to the dolerite hills that bound the northern margin of the study area. Lastly, it forms a single outcrop, about 11,032 m^2 in size, where it mantles the tail leading away from the crag described above. The drift overlies Friis II near the center of the paleovalley, whereas it rests on granite and dolerite bedrock along both the north and south paleovalley walls (Figure 3.1). It underlies Cavendish III throughout the study area. At the ground surface the drift forms a bench that exhibits a 1 to 2 m slope. This slope leads down to bedrock except near the center of the paleovalley where it leads down to Friis II. Weathered black dolerite boulders and the black to dark-reddish colored grus they produce characterize the surface of Friis I.

Granite bedrock adjacent to Friis I shows two distinct sets of striations. Based on crosscutting relationships the older set is oriented at 029°, nearly parallel to the axis of the paleovalley, whereas the younger set is oriented at 099° (Table 3.3). The older striations emerge primarily from beneath Friis II but at two locales a striated surface emerges from beneath Friis I. These striations are found only within 10 m of drift edges, whereas the younger set of striations is found 10 to 20 m father from drift edges. Where Friis I rests on sandstone bedrock in the northwest of the study area, along what would have been the northern wall of the paleovalley, the till includes a basal horizon of crushed rock above jointed and disaggregated sandstone. This horizon includes slabs of the underlying sandstone, some of which hold striations. Nearly all of these slabs are oriented with long

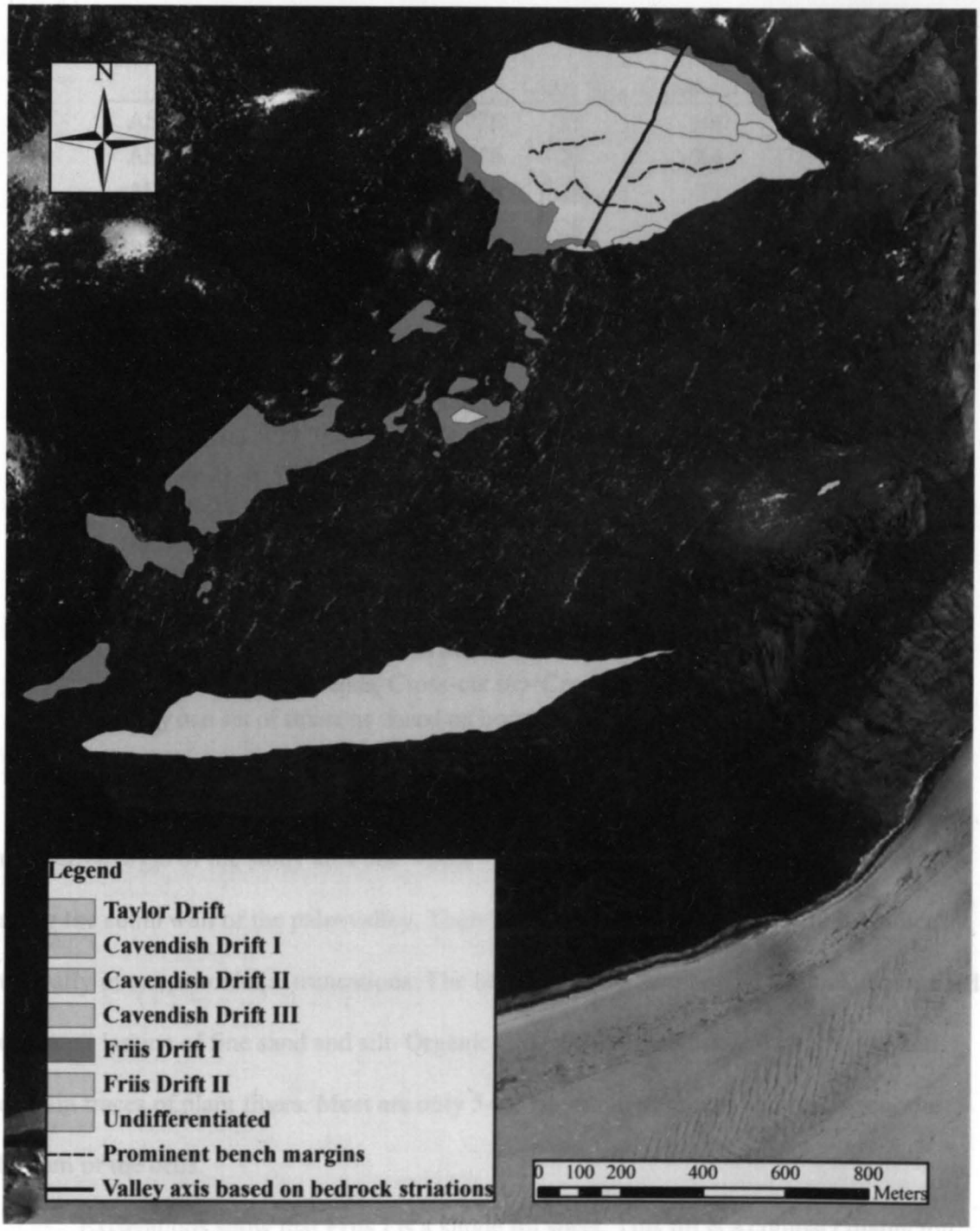

Figure 3.14. Outcrop map of Friis I. All other units shown in gray.

axes northeast-southwest and upper surfaces dipping to the southwest. Striations on these slabs are also oriented northeast-southwest.

Table 3.3. Location and orientation of striations documented in the eastern Friis Hills.

Site	Coordinates	Older Str.	Cross-cut str.
ASE-10-07	77.75033; 161.57776	25	100
ASE-10-07	77.75033; 161.57776	25	84
ASE-10-07	77.75033; 161.57776	28	77
ASE-10-07	77.75033; 161.57776	28	81
ASE-10-07	77.75033; 161.57776	29	*
ASE-10-07	77.75033; 161.57776	32	107
ASE-10-07	77.75033; 161.57776	37	87
ASE-10-01	77.75610; 161.53632	*	109
ASE-10-03	77.74660; 161.56856	*	150
ASE-10-06	77.75477; 161.56470	*	72
ALS-06-21-6	77.74624; 161.56910	*	115
ALS-06-21-7	77.74656; 161.56846	*	105
ALS-06-22	77.75742; 161.51386	*	105
Mean		29	99

Coordinates are latitude south and longitude east.
Orientations are in degrees from true North.
Older str.=Older striations; Cross-cut str.=Cross-cutting striations
*Only one set of striations found on bedrock.

Fossil-bearing fluvial and lacustrine beds cap Friis I where it crops out along the northern margin of the study area and where it emerges from beneath overlying tills sheets along the south wall of the paleovalley. These beds are rare and crop out only sporadically, typically in steep erosional truncations. The beds are a maximum of 1.2 m thick, comprised of planar lamina of fine sand and silt. Organic beds are dark reddish-brown in color and contain traces of plant fibers. Most are only 5- to 10- cm in thickness and occur near the bottom of the beds.

Excavations show that Friis I is a single till sheet. This till is a compact diamicton comprised of mostly cobble-size clasts of dolerite, granite, sandstone, and siltstone set within a muddy, sandy gravel matrix (Figure 3.15; Tables 3.1, 3.2). Among the 348 clasts analyzed, two clasts from the till are erratic. One is a fine-grained, white plagioclase-rich

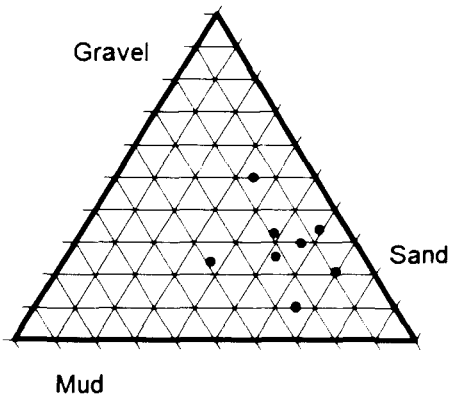

Figure 3.15. Ternary plot of Friis I matrix. Based on Folk (1974), the average of the matrices analyzed plotted as muddy sandy gravel. Scales go from 0 to 100%. 100% rests at labeled points; 0% rests at line opposite point.

granite and the other is coarse-grained, feldspar-rich granite. About 25% of the clasts are molded. Friis I has the highest percentage of sandstone clasts at 13.4% but this figure is skewed by a high number of bedrock fragments present where the till rests on sandstone bedrock. A few weakly stratified beds are present within excavations in the till as well as a few thin interbeds of sand and gravel (Figure 3.16). Most of these interbeds are 30- to 80-cm thick.

The till shows evidence for prolonged surface weathering. Cement binding sand grains in sandstone clasts have been chemically weathered to depths of as much as 40 cm causing clasts to disintegrate once they are exposed in excavations. Nearly all dolerite boulders exposed at the ground surface have been eroded to become level with the ground surface; most are surrounded by halos of grus that extend as much as 4 to 5 m to the northeast.

Interpretation. Friis I rest stratigraphically below Cavendish III and above Friis II. It is interpreted primarily a basal lodgement till based on the level of compaction seen in most pits. Where the till is thickets, decreasing compaction upward suggests that some horizons in the unit may be basal ablation tills with the interbeds of sand and gravel representing either subglacial or proglacial flow of meltwater. Based on muddy matrix

Figure 3.16. Excavation pit of Friis I. Pit is a dolerite-rich till that coarsen upwards. Sandstone "ghosts" can be seen in the image as white patches on the pit walls.

texture and the presence of striated clasts, the till was deposited by wet-based ice. Erratic clasts indicate that ice could have originated outside of the Friis Hills. An alternative hypothesis is that the erratics could have been from a rock unit near the Friis Hills, which has now been eroded away.

Based on two striated bedrock surfaces adjacent to Friis I, ice flowing roughly parallel to the paleovalley axis deposited the till. The orientation of striations on slabs of sandstone bedrock within the till and the preferred orientations of some clasts also suggest ice flow parallel to the valley axis. Identical striations beneath Friis II could complicate this interpretation but the simplest explanation is that ice depositing both Friis I and Friis II flowed in directions that were indistinguishable from each other. This means that striations oriented at 025° to 037° represent flow of ice for both Friis I and Friis II. The crosscutting striations oriented east-west are most likely associated with deposition of Cavendish III. This makes sense if glaciers flowing in the same direction as those depositing Cavendish III were responsible for the partial erosion of underlying units evident in outcrop patterns.

Fossil-bearing fluvial and lacustrine beds that cap Friis I were deposited during an ice-free period. Organic content in some beds suggests they are peats that formed in wet, low-lying areas where surface water collected and encouraged plant growth. Their rare and patchy distribution could also suggest that they were eroded by ice depositing overlying drifts.

Friis I's location in the paleovalley, along the northern bluffs, and as blanket covering the tail at the western edge of the study area, provides evidence that Friis I once blanketed much of the eastern Friis Hills. However, ice crosscut the paleovalley and eroded away much of Friis I. Only isolated remnants of Friis I, most of which were protected by dolerite bedrock ridges, were left as relics. Dolerite boulders eroded to the ground surface and sandstone "ghosts" suggest that Friis I is one of the oldest tills in the paleovalley.

Friis II

Characteristics. Friis II is a 1-to 2-m-thick, compact, light gray (2.5Y 7/1) diamicton with a capping horizon of bedded sand and gravel. Friis II is the lowest stratigraphic unit filling the paleovalley and the oldest map unit in the eastern Friis Hills (Figure 3.1). The drift crops out in two locales: 1) along the southern edge of the valley fill where it emerges from beneath Cavendish III to form a narrow bed between the bedrock and overlying till and 2) at the western edge of the valley fill where it extends westward for 10 to 20 meters from beneath Friis I (Figure 3.17). The drift forms a bench 1 to 1.5 m high that terminates at a steep erosional truncation. Throughout the study area Friis II rests on bedrock. The southern outcrop mantles the southern wall of the paleovalley, whereas the western outcrop fills the lowest portion of the paleovalley. Striated and polished bedrock is common beneath the till and on bedrock exposed adjacent to till edges. Striations beneath the till are oriented between 025° and 037°. As described above, those found more than about 10 meters from the till include crosscutting striations averaging 096° (Table 3.3).

The basal horizon of Friis II is comprised of a single, relatively thin till sheet. It is a dense, dark gray in color, strongly consolidated till that has been plastered onto granite bedrock (Dreimanis, A., 1989). In all excavations the till sheet is from 0.5 to 1.4 m thick. Cobble and boulder-sized clasts in the till are rare with most being only gravel sized or smaller. Clasts are composed of dolerite, granite, and sandstone. The till matrix is gray to dark gray, gravelly, muddy sand (Figure 3.18; Table 3.1). Friis II has the highest percentage of erratic clasts among the analyzed map units. All of these erratics consist of fine-grained, light gray granites that are notably dissimilar to local granite bedrock. Despite resting on striated bedrock, the percentage of striated clasts in the till is minimal but

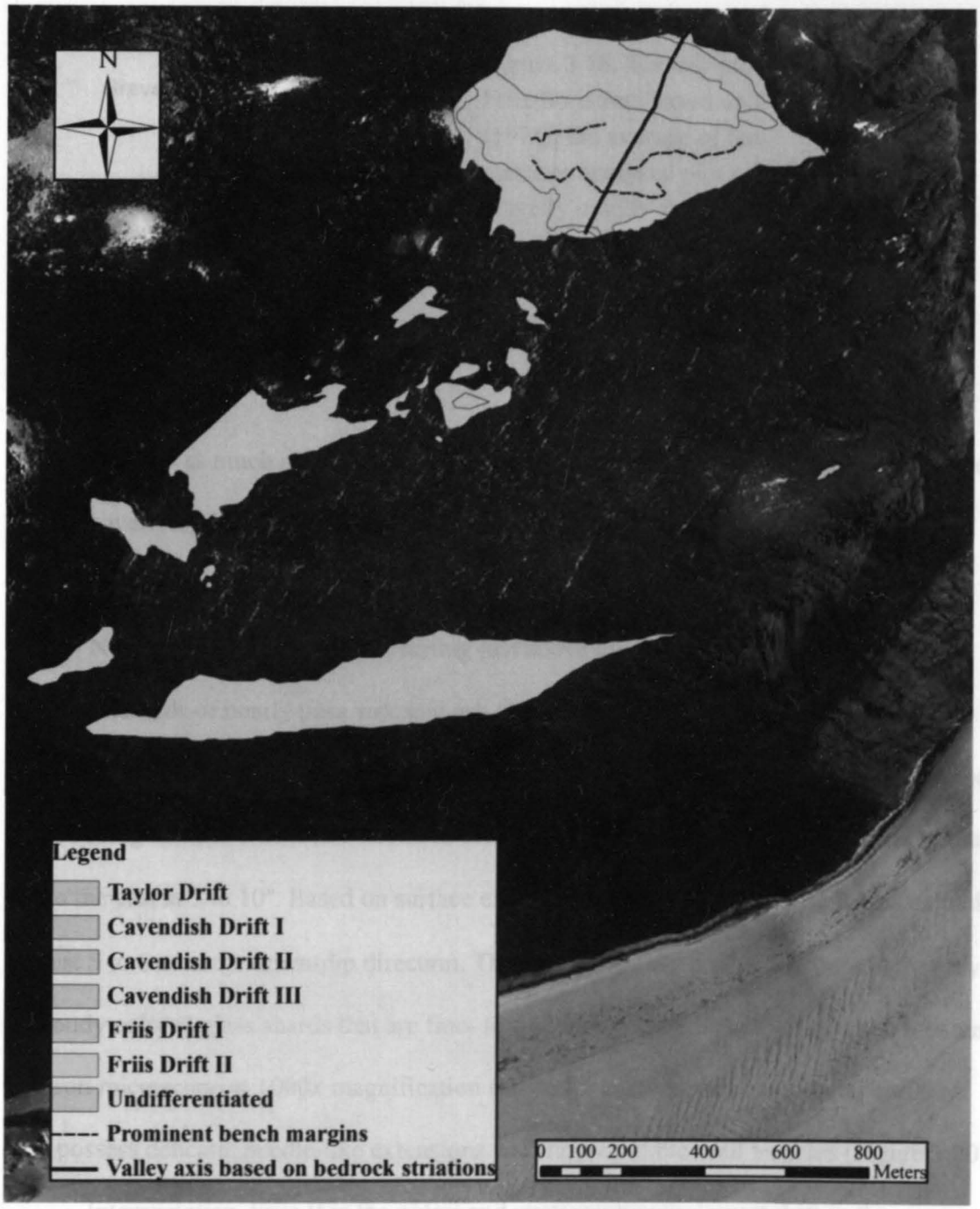

Figure 3.17. Outcrop map of Friis II. All other units shown in gray.

molded and polished clasts are common (Table 3.2).

Above the basal horizon the unit grades upward to bedded sand and fine gravel, both of which are light brown in color. These beds combined are less than 1 m thick. They

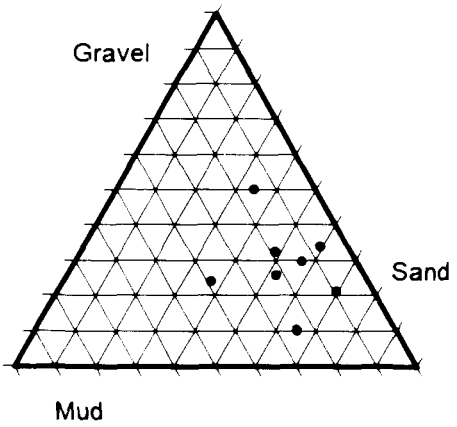

Figure 3.18. Ternary plot of Friis II matrix. Based on Folk (1974), the average of the matrices analyzed plot as gravelly muddy sand. Scales go from 0 to 100%. 100% rests at labeled point; 0% rests at line opposite point.

extend laterally as much as 10 m where they either meet the paleovalley side walls or taper beneath overlying Friis I. The sand and gravel beds are less consolidated than the underlying till but are still more consolidated than any other unit filling the paleovalley.

Near the base of these beds, resting just above the till, are several small, lens-shaped interbeds of nearly pure volcanic ash (Figure 3.19). Each lens is from 3 to 40 cm thick and extends in cross-section from 30 to 80 cm. Because of the uniform texture of the ash, bedding in these lenses is difficult to discern but several show faint planar lamina that dip to the east at 5 to 10°. Based on surface exposures of volcanic ash, these lenses extend at least 5 to 6 m in the down-dip direction. The ash is comprised of nearly pure, light gray to cloudy colored glass shards that are fine- to coarse-sand sized. Analysis using a scanning electron microscope at 1000x magnification showed that ash shards are angular and that they possess delicate, needle-like extensions and fragile bubble-wall vesicles (Figure 3.20).

Interpretation. Friis II is the oldest and stratigraphically lowest drift in the paleovalley. The lower horizon is interpreted as a lodgement till deposited at the bed of a glacier that flowed to the northeast, down the axis of the paleovalley. The glacier was wet-based given the muddy till matrix, molded and polished clasts, and striated bedrock. Since

Figure 3.19. Nearly *in-situ,* bedded volcanic ash interbeds in Friis II.

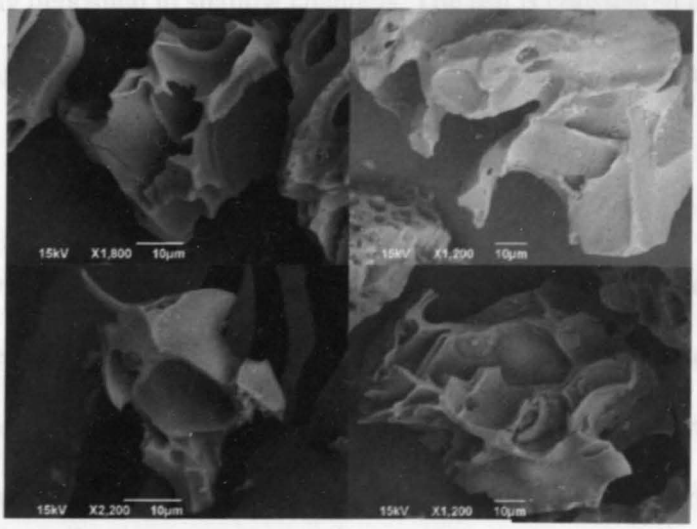

Figure 3.20. SEM images of volcanic ash glass shards.

Friis II till rests directly on striated bedrock, the simplest explanation is that Friis II till rests directly on striated bedrock, the simplest explanation is that ice depositing Friis II also cut the paleovalley. Friis II has the lowest concentration of clasts per kg (10), but it has the highest percentage of granite clasts compared to the other four units at 13% (Table 3.2). This is because Friis II was deposited directly on granite bedrock as the paleovalley was being formed. It also has the most erratic clasts among all of the tills at 3.4%. This could suggest that Friis II came from a distant source region, however, these erratics may actually be from bedrock that cropped out near the Friis Hills before extensive erosion. Ice flow was likely to the northeast at 025°-037°, based on striated bedrock beneath and adjacent to the till. The till was probably deposited when the ice entered a depositional phase after cutting the paleovalley. The upper horizon in the drift represents an ablation phase. As the ice melted, beds of sand and gravel were deposited along the ice margin.

The volcanic ash, which has been dated at 19.76 ± 0.07 Ma (Sidney Hemming, preliminary lab report from Lamont-Doherty Earth Observatory), likely fell on the surface of the glacier depositing Friis II during the ablation phase. It quickly flowed off in melt-water before being deposited in shallow channels. The ash is considered nearly in-situ because of the angular shards of glass and minimal occurrence of other lithic grains.

Taylor Drift

Characteristics. Taylor Drift is a veneer of scattered dolerite boulders and cobbles that sit on surfaces of granite bedrock and grus. It ourcrops on surfaces along the southern rim of the eastern Friis Hills. In map view it forms a narrow band that parallels the margin of Taylor Glacier and it covers an area of 173,025 m^2 (Figure 3.21). The dolerite clasts

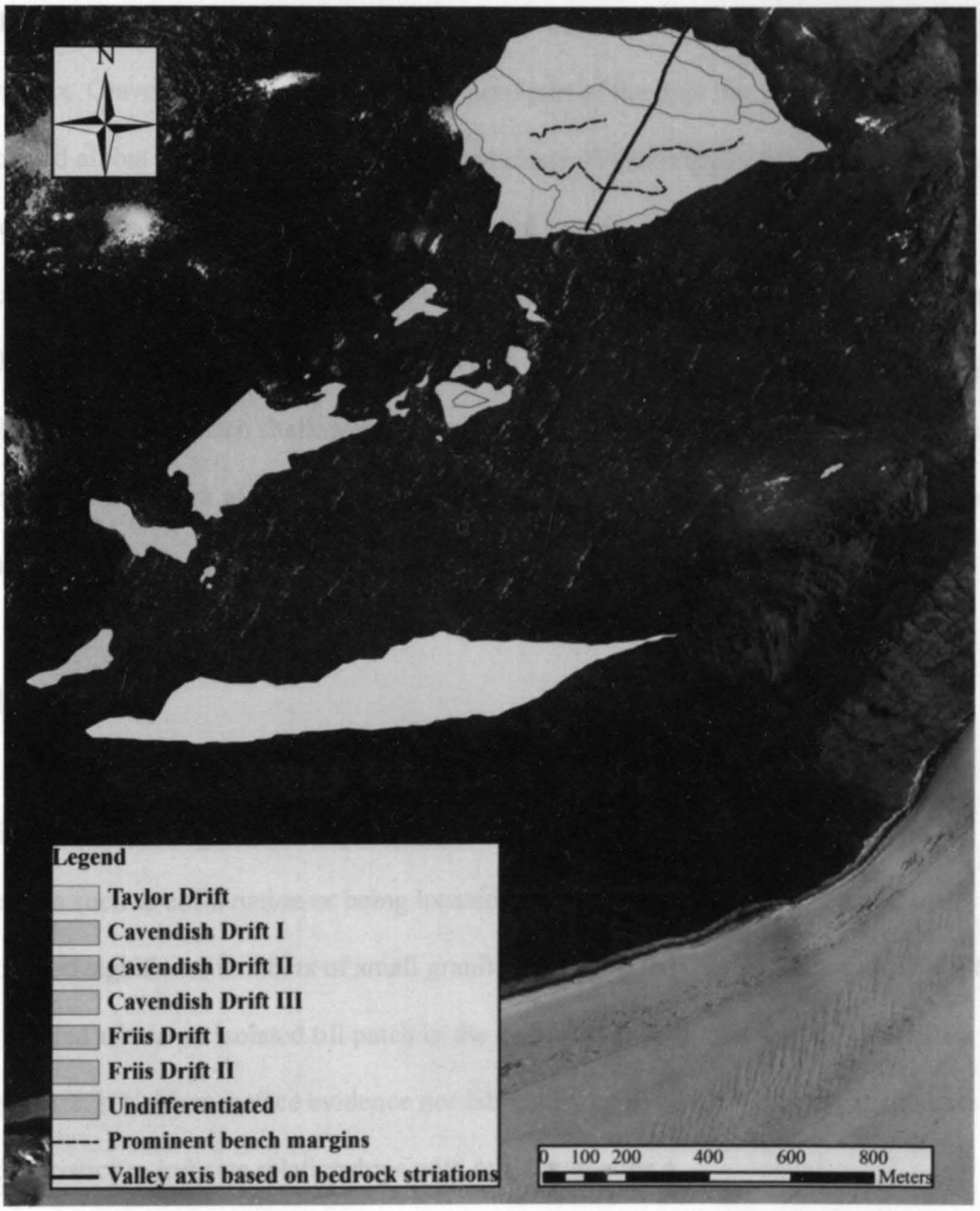

Figure 3.21. Map of Taylor Drift in light green located in the southwest corner of the eastern Friis Hills. All other drifts shown in gray.

comprising the drift are weathered reddish-brown in color and all display pitted and stained, weathered surfaces.

Interpretation. Taylor drift is likely the youngest till in the eastern Friis Hills but its stratigraphic relationship to the other drifts in this study is unknown. A cold-based glacier

likely deposited this drift because it contains only weathered dolerite boulders and has no till matrix. Gravel and sand may have once been part of the drift but subsequent erosion has destroyed all but the largest and most resistant clasts. Weathering of the dolerite boulders indicates that they have been exposed to subaerial processes for a long period. This till was probably deposited from an expanded Taylor Glacier. Being as much as 500 m above the surface of the modern glacier, the till might date back to a time when the trough holding Taylor Glacier was much shallower than it is today. It is unlikely that Taylor Glacier has been sufficiently thick at any time in the past 3 to 5 million years to deposit the till based on nearby glacial geologic studies (Brook et al., 1993; Willenbring et al., 2006).

Undifferentiated

Five samples analyzed, 10-43A/B, 10-64, and 10-74A/B, were classified as undifferentiated. Samples 10-43A/B and 10-74A/B were influenced by down-slope processes such as colluviation or being located directly above weathered bedrock that introduced significant numbers of small granite clasts to overlying sediments. ASE-10-64 was located within an isolated till patch in the eastern corner of the eastern Friis Hills (Figure 3.22). Neither surface evidence nor laboratory analysis provided any diagnostic characteristics to indicate relationships with other map units.

Statistical analyses of drifts

Sedimentological drift characteristics were analyzed for statistical significance. Using the statistical program SAS 9.4, analysis of variance (ANOVA) for means with an alpha level of 0.10 was determined. The null hypothesis is that the means of the

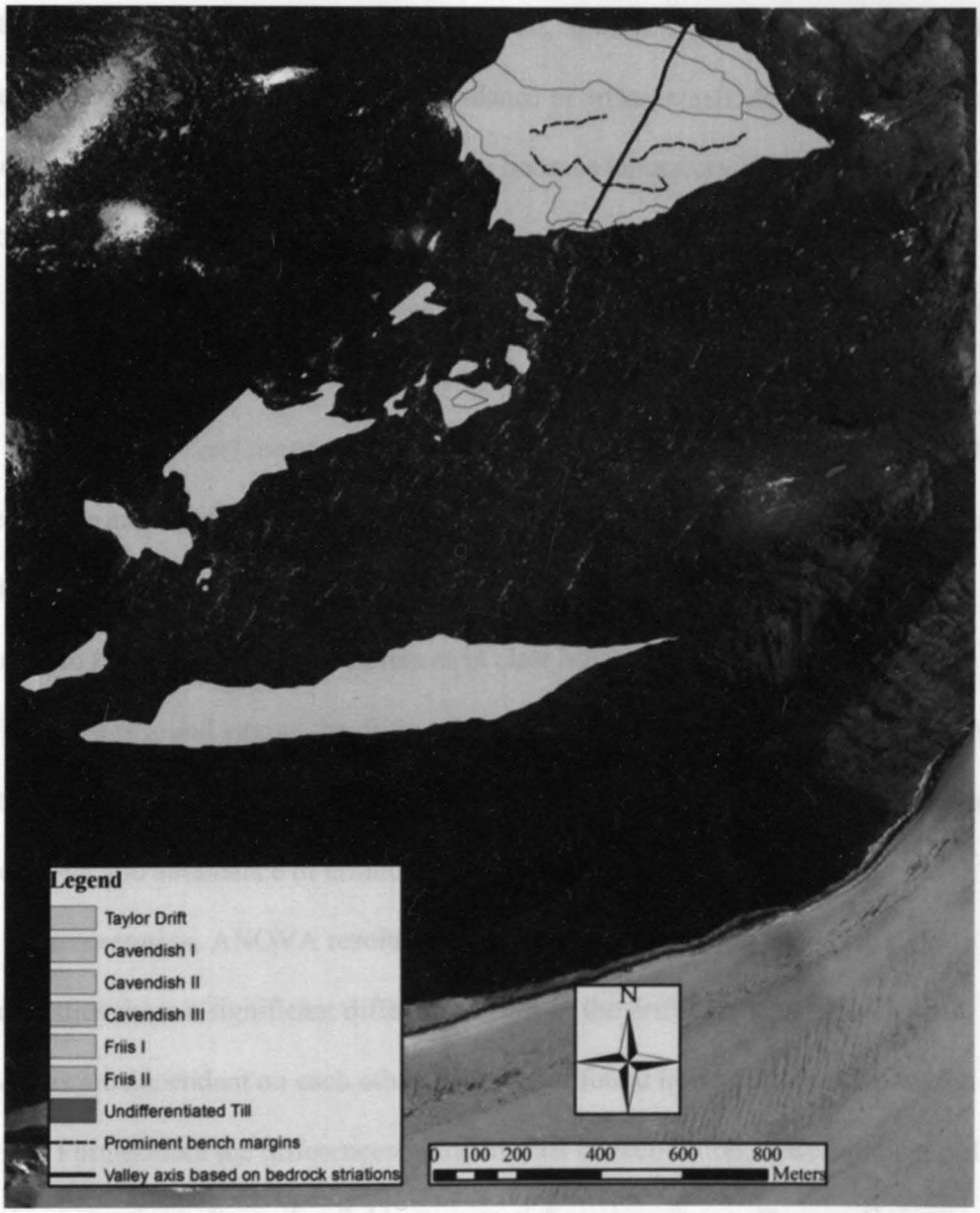

Figure 3.22. Map of isolated patch of undifferentiated drift in the south-eastern corner of the eastern Friis Hills.

sedimentological drift characteristics are the same, therefore rejecting the null hypothesis means that the drifts are significantly different. An alpha value of 0.10 indicates that 10% of the time a false rejection of the null hypothesis could be accepted. If a P-value of 0.10 or lower is calculated, then the means are significantly different and a false rejection is

unlikely. Means compared were % gravel, % sand, % mud, clasts/kg, and dolerite, granite, and sandstone clast abundance and the abundance of erratic clasts. Means from Cavendish I were excluded from the statistical comparison because laboratory data are available for only two samples.

Results for differences in the mean values of gravel, sand and mud in drift matrices produced a P-value of 0.1285, 0.7454, and 0.0747, respectively (Table 3.4). The high P-value for gravel and sand means no significant difference was found between the drifts. However, the means of percent mud had a P-value below the alpha value, which means that this characteristic is significantly different among the four drifts. ANOVA was also computed to test for significant differences in clast lithology and clast texture. No significance was found among the drifts on the basis of percent dolerite, granite, sandstone and striated clasts (Table 3.4). In contrast, results for clasts/kg, percent of clasts molded and polished, and abundance of erratic clasts had P-values below the alpha level.

Interpretation. ANOVA results for means of sedimentology and clast characteristics show a significant difference between the drifts. Because gravel, sand, and mud values are dependent on each other, differences found in mud support separation of the drifts. Furthermore the differences found in clast concentration, clast molding, polish and percent erratics indicate that field interpretations were correct. Duncan Grouping results for eastern Friis Hills drifts are in Appendix E.

Table 3.4. ANOVA table of P-values and significant difference found for the means of the drift characteristics.

Characteristic	P-value	Sig D
Gravel	0.129	N
Sand	0.41	N
Mud	0.075	Y
Clasts/kg	0.092	Y
Dolerite	0.339	N
Granite	0.312	N
Sandstone	0.585	N
Striated	0.373	N
Molded	0.071	Y
Polished	0.013	Y
Erratic clasts	0.002	Y

Alpha value=0.10
Abbreviations: Sig D=Significance Difference found between drift means,
Y=significance found, N=no significance found.
Means from Cavendish I were excluded because of small sample sizes.

CHAPTER 4. DISCUSSION

The primary objective of this study was to define a stratigraphic column for tills in the eastern Friis Hills. Field observation and GPS elevation analyses showed that these tills form a sedimentary sequence 35 m thick. The first step toward organizing these sediments into a stratigraphic column was to divide them into units based on differing physical characteristics, which correspond to differing depositional environments or processes.

Based on field observations the sedimentary sequence in the eastern Friis Hills has been divided into two drift packages, which I have named in this thesis Friis drift and Cavendish drift. At the ground surface differences between the two are evident. Friis drift has low relief and gradual surface slopes; the drift surface is dark because of widespread dolerite grus and because subaerial erosion has obliterated granite and sandstone boulders at the ground surface. In contrast, Cavendish drift shows distinct benches bounded by steep erosional truncations; the drift surface is light in color because of scattered, upstanding granite and sandstone clasts. Other differences were obvious in excavations. Friis drift is comprised primarily of two compact lodgement tills that contain erratic clasts. Cavendish drift is comprised less compact ablation tills that contain very few erratic clasts.

Laboratory analyses provide quantitative evidence to support the division of the eastern Friis Hills sedimentary sequence into two main drift packages (Tables 3.1 and 3.2). ANOVA results showed that several of the differences between mapped drifts were statistically significant. Generally, studies have shown that differences between drifts result primarily from differences in bedrock lithology of source regions, transport pathways and distances, and depositional environments (Boulton, 1978; Kjaer, 1999).

Interpretation of differences among glacial geologic units

The differences between Friis drift and Cavendish drift can be traced back to depositional environment and process, and to differing source regions or transport distances. First, small alpine glaciers deposited Friis drift. Supporting evidence comes from the broad and shallow cross-section of the paleovalley and its smooth, U-shaped cross-sectional profile. In contrast, tills in Cavendish drift were deposited by a much larger glacier than that depositing Friis drift. The ice did not follow the previously established ice flow pattern. It likely flowed over the terrain, ignoring the paleovalley that had confined Friis ice. Corroborating evidence comes from striated bedrock surfaces. Those beneath Friis drift are oriented parallel to the paleovalley axis, which trends northeast. All striations found in association with Cavendish drift are oriented east-west. Moreover, along the western margin of Friis II, these east-west striations crosscut those oriented to the northeast. Cavendish ice also deposited much thicker sedimentary sequences. Cavendish III is 15 m thick compared to a total thickness of only 12 m for Friis drift.

Evidence for meltwater also suggests differences between the two drifts. Friis drift includes only a few thin interbeds of sand and gravel set in ablation-till facies that are no more than 1 m thick. In contrast, Cavendish drift has abundant evidence for high volumes of meltwater being present during deposition. An example of this is in Cavendish III, which includes ablation tills 3 to 4 m thick, and 2 to 3 m thick cross-beds of sand and gravel.

Information regarding the relative geographical size of the Friis and Cavendish glacial systems and their possible source regions comes from clast lithology. Erratic clasts are generally the most useful for determining ice source regions and are commonly used for this purpose (Gwyn and Dreimanis, 1979). Unfortunately, bedrock maps do not exist for

most regions adjacent to the Friis Hills because of thick ice cover. Moreover, because of extensive glacial downcutting, entire bedrock sources that may have been adjacent to the Friis Hills during deposition could now be non-existent. For these reasons and because the percentage of erratic clasts in drifts from the Friis Hills is very small (< 1%), little importance is assigned to erratic clasts.

An obvious difference in drifts from the Friis Hills is that sandstone clasts are twice as abundant in Friis drift as they are in Cavendish drift. Correspondingly, dolerite clasts are more abundant in Cavendish drift than in Friis drift. This variation has little to do with differences arising from local bedrock. First, granite, sandstone and dolerite bedrock crop out adjacent to one another over short distances in the Friis Hills and throughout the Dry Valleys region. Second, because dolerite sills and sandstone formations are oriented horizontally and they rest on granite above a roughly horizontal contact, their outcrop patterns are repeated over and over again in hills and valleys throughout the region. Together this means that all glaciers in this region, with the possible exception of small niche glaciers, could be expected to carry similar rock populations. Given this, the differences in sandstone versus dolerite percentages in drifts may have to do with transport distance. Sandstone is a weak rock relative to dense dolerite. With increasing distance from the source, sandstone clasts would be more likely to be crushed or abraded. Following this reasoning, the high percentage of sandstone clasts in Friis drift implies that it experienced relatively shorter transport distances than did any of the tills in Cavendish drift. This conclusion supports the hypothesis that glaciers depositing Friis drift were likely small and confined to valleys, whereas glaciers depositing Cavendish drift were large enough to ignore these landscape features.

In summary, an interpretation of drift characteristics combined with ice flow patterns suggests that tills in Friis drift were deposited from small alpine glaciers, whereas tills in Cavendish drift were deposited from large, unconfined glaciers. Evidence for this interpretation includes 1) Friis glaciers followed the topography of the paleovalley, 2) tills in Friis drifts are relatively thin, 3) sandstone clasts in Friis drift survived relatively short transport distances and 4) fluvial and proglacial deposits in Friis drift are limited in extent. Cavendish drift more likely represents a large, unconfined glacier system such as an ice cap because 1) glacier ice ignored and crosscut the paleovalley, 2) it deposited thick tills along a fluctuating margin, 3) rare sandstone clasts suggest relatively long transport distances, and 4) prolonged melting produced thick sequences of proglacial fluvial beds.

Glacial History and Chronology

1. Cutting of a small glacial valley and deposition of Friis II. The oldest known event for which evidence is preserved is the cutting of a small paleovalley through the Friis Hills (Figure 4.1A). Although it is unclear if the paleovalley was originally formed by a fluvial system, its classic U-shape, smooth valley walls, and striated bedrock surfaces all indicate that glacial erosion expanded the paleovalley. After eroding the valley form, the ice shifted to a depositional phase and Friis II was deposited. The ice plastered this dense lodgement till on the valley floor indicating it was still actively flowing as deposition took place. After this, ice margins retreated and thin beds of well-sorted sediments began to be deposited on the valley floor. After only a small thickness of beds accumulated, volcanic ash fell on or along ice margins. It quickly flowed off the ice before being deposited in small melt-water channels on the valley floor. The distance traveled from its original location was short

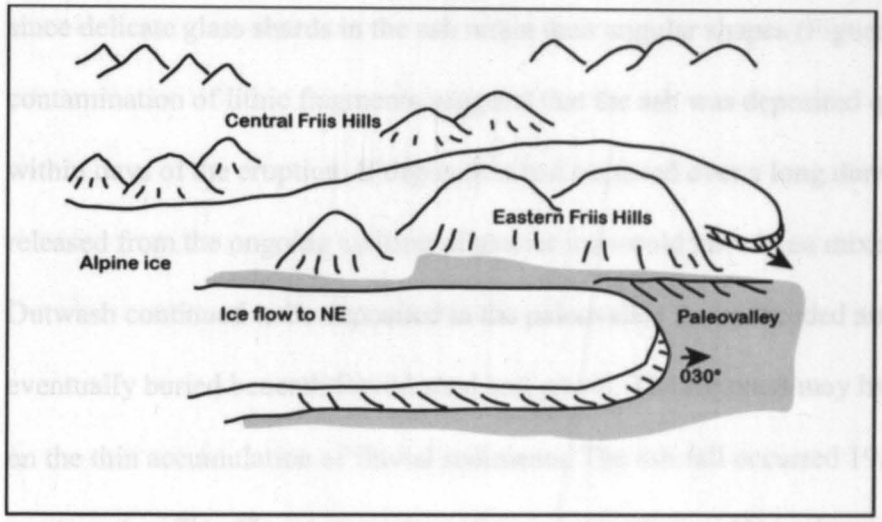

A. 20 Ma ago alpine ice flowed over the eastern Friis Hills and began to cut and fill the paleovalley with Friis drift. Interbedded in the Friis drift are paleosols and volcanic ash.

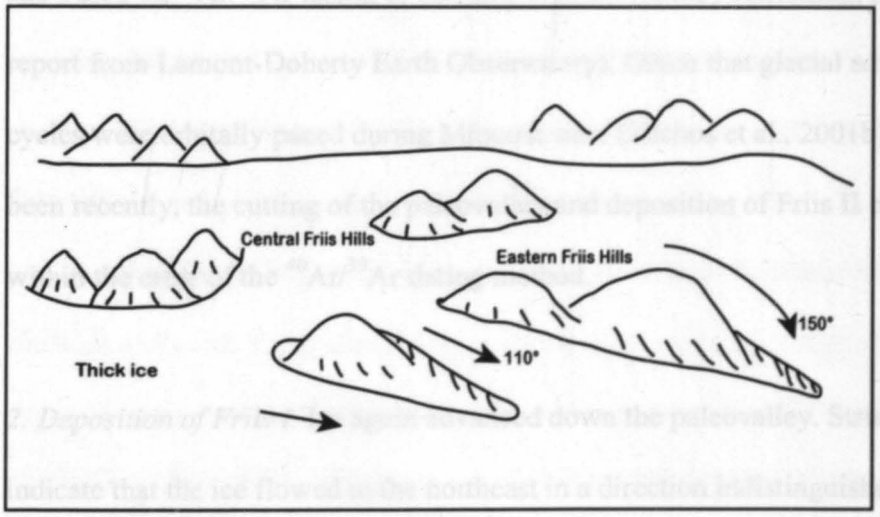

B. 19-14 Ma ago thick ice flowed through the Friis Hills. This ice cross-cut the paleovalley, eroded tills and striated bedrock. Cavendish drift was deposited along the ice margin. A maximum ice configuration is shown.

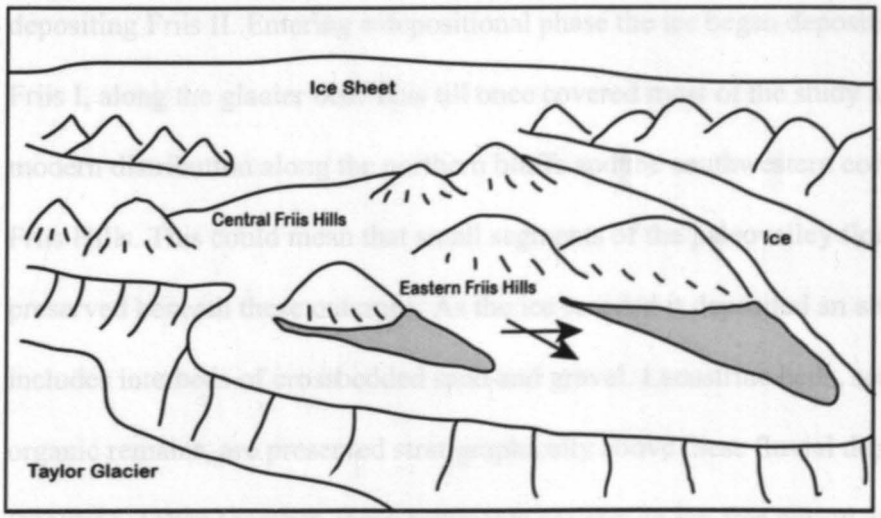

C. After depostion of Cavendish drift, ice downcuts adjacent to the Friis Hills. This isolated the Friis Hills and eroded high-elevation terrian that may have previously been an ice source (as in A).

Figure 4.1. Illustration showing hypothesized ice configuration for different times.

since delicate glass shards in the ash retain their angular shapes (Figure 3.20). Minimal contamination of lithic fragments suggests that the ash was deposited quickly, possibly within days of the eruption. If deposition had occurred over a long duration, sediment released from the ongoing melting of glacier ice would have been mixed with the ash. Outwash continued to be deposited in the paleovalley as ice receded and the ash beds were eventually buried beneath fluvial sand and gravel. The ice mass may have been small based on the thin accumulation of fluvial sediments. The ash fall occurred 19.76 Ma (± 70,000) ago based on $^{40}Ar/^{39}Ar$ dating of sanidine crystals (Sidney Hemming, preliminary lab report from Lamont-Doherty Earth Observatory). Given that glacial advance and retreat cycles were orbitally paced during Miocene time (Zachos et al., 2001b), just as they have been recently, the cutting of the paleovalley and deposition of Friis II could have occurred within the error of the $^{40}Ar/^{39}Ar$ dating method.

2. Deposition of Friis I. Ice again advanced down the paleovalley. Striations on bedrock indicate that the ice flowed to the northeast in a direction indistinguishable from that depositing Friis II. Entering a depositional phase the ice began depositing a lodgement till, Friis I, along the glacier bed. This till once covered most of the study area given its wide modern distribution along the northern bluffs and the southwestern corner of the eastern Friis Hills. This could mean that small segments of the paleovalley floor and walls are preserved beneath these outcrops. As the ice receded it deposited an ablation till which includes interbeds of crossbedded sand and gravel. Lacustrine beds, some of which include organic remains, are preserved stratigraphically above these fluvial deposits in a few localities. Taken together, these sediments register an ice-free period after the retreat of

glacier margins from the paleovalley. These deposits are younger in age than the volcanic ash used to date Friis I. However, the time separating the deposition of Friis II from the deposition of Friis I was likely short given the lack of a weathering horizon and soil development between the two drifts. Deeply weathered clasts and sandstone ghosts within the till support an ancient age for the till.

3. Deposition of Cavendish drift. After an ice-free period of undetermined duration, ice again flowed through the Friis Hills. It flowed to the east, at an orientation of about 099°, ignoring the previously established southwest-northeast flow pattern. It removed as much as 35 m of bedrock from the eastern Friis Hills based on the difference in elevation between the bedrock hills and the glacially eroded granite plateau (Figure 4.1B). Based on km-scale molding of topography it surrounded the dolerite hills that bound the study area to the west and north. Cavendish III represents the advance and retreat of this ice at least four times. Fine-grained fluvial deposits in the drift register periods of reduced ice extent. Coarsening-upwards fluvial sequences capped by debris flows register ice advance, each of which culminates in the deposition of a 1- to 3-m thick till sheet. These were likely deposited along a lateral ice margin given that molded bedrock shows flow to the east, whereas fluvial beds and debris flows show flow to the northeast. Both Cavendish I and II represent the advance of thick ice over the study area sometime after deposition of Cavendish III. An erosional truncation beneath Cavendish I indicates that ice shifted from a depositional to an erosional phase and back again at least once.

4. Glacial erosion and the molding the Friis Hills surfaces. A major unknown concerns the

timing of glacial erosion relative to the deposition of Cavendish drift. In one scenario, deposition of Cavendish drift occurred before the major erosional phase that streamlined bedrock surfaces in the Friis Hills and crosscut the paleovalley. In this scenario glacial cutting might take place long after deposition of Cavendish drift and it may previously have been much more extensive. The present margins of Cavendish I, II, and III would therefore represent erosional truncations. In an alternative scenario, cutting at the glacier bed could have taken place at the same time the drift was being deposited along, and in the case of till sheets, beneath the ice margin. Margins of Cavendish I, II, and III would roughly correspond to ice margins.

In either of these two scenarios, ice flowed around the upstanding dolerite hills to the north and west of the study area. Directly down-flow from the northern hills the segment of the paleovalley and Friis drift were preserved (Figure 4.1B and 4.1C). Likewise, Friis I was preserved behind the dolerite-capped hills at the western edge of the study area (Figure 1.3). Ice flowing over the saddle between these knolls cut the 35-m-deep glacial trough that bisects the eastern Friis Hills. Based on the crosscutting of Friis I and the enclosed ash beds, downcutting took place after 19.76 Ma.

5. The topographic isolation of the Friis Hills. After glacial ice molded and streamlined the upper surfaces of the plateau, erosion continued and several hundred meters of bedrock were removed to create deep glacial troughs both to the north and south of the Friis Hills (Figure 4.1C). This was accomplished through the process of selective linear erosion (Sugden and John, 1976). Selective linear erosion occurs where ice initially cuts a shallow trough, which then allows for increased flow of ice through the trough. This increased ice

flow produces a local increase in erosion. As the trough becomes deeper ice flow becomes concentrated. The glacier begins to funnel ice through the trough resulting in a positive feedback loop. Based on the orientation of narrow troughs to the north and south of the Friis Hills this occurred when ice flowed to the east, roughly parallel to that depositing Cavendish drift. The end result of this selective linear erosion was the topographic isolation of the Friis Hills and an extreme example of topographic inversion. Deep troughs could now be positioned where high-elevation source areas once fed glaciers depositing Friis drift. These tills and the paleovalley mark a valley floor that now sits high above surrounding topography. This is not uncommon in the Dry Valleys. Small segments of alpine glacial valleys have been mapped on mountaintops at elevations as high as 3000 m on Mt Fleming and Mt Feather (Hicock et al., 2003; Stroeven and Prentice, 1997).

There is no direct evidence of when the Friis Hills became isolated, however glacial records from the Asgard and Olympus Range show that Antarctic ice thickened and expanded sometime between 13 and 14 Ma ago (Marchant et al., 1993; Lewis et al., 2006; 2007). This expansion coincided with climate cooling between 13.9 and 14.1 Ma, which was significant enough to cause the local extinction of tundra plants and animals and to cause alpine glaciers to shift from wet- to cold-based thermal regimes (Lewis et al., 2007, 2008). Antarctic near-shore marine records register a cooling in surface waters and in some locales an expansion of Antarctic ice between 13.7 and 13.9 Ma (Shevenelle et al., 2004, 2008). All of these events have been correlated to the globally important Mid-Miocene Climatic Optimum. Given these dated records, the cutting and isolation of the Friis Hills probably took place approximately 14 Ma ago. With the dated ash interbeds from Friis II, downcutting is therefore bracketed between 14 and 19.76 Ma ago.

Based on glacial geologic studies from nearby high-elevation valley floors, Taylor Glacier has not been thick enough to deposit Taylor drift at these elevations for 3 to 5 Ma (Brook et al., 1993; Willenbring et al., 2006). This means Taylor drift is 14 to 5 Ma old. Because it is a coarse-grained till lacking evidence for molded clasts or a mud-rich matrix, it was deposited after the transition to cold-based glacial thermal regimes (Lewis, 2007).

An important consequence of the topographic isolation of the Friis Hills coupled with the climate change is the preservation of deposits on the plateau surface. Once downcutting confined eastward-flowing ice to deep troughs, drifts on the plateau surface were protected from erosion beneath expanded outlet glaciers. And, because of the transition to a cold climate, alpine glaciers building up in the Friis Hills would be cold based and non-erosive (Cuffey et al., 2000). The only agents of erosion active in this environment are subaerial, such as wind and salt weathering, but extremely low erosion rates enabled the preservation of Miocene glacial deposits on the plateau surface.

Wider Implications

Tills in the eastern Friis Hills and paleovalley are between 20 and 14 Ma old, which means they were deposited prior to the Mid-Miocene Climate Transition. The dating suggests that they may have been deposited during or just before the Mid-Miocene Climatic Optimum (17 to 15 Ma), a period for which terrestrial climate evidence in Antarctica is entirely lacking. This means that temperature estimates from fossils preserved in the eastern and central Friis Hills are uniquely important indicators of paleoclimate. This study is a first step in the dating of these fossils because the Ar-dated stratigraphic column for the eastern Friis Hills could be correlated to one constructed for the central Friis Hills.

Friis drift and the morphology of the paleovalley are consistent with a small-scale alpine glacial system. This indicates that a modern-sized East Antarctic Ice Sheet was not overtopping the Transantarctic Mountains 20 Ma ago. Cavendish drift indicates that glacier systems grew in size after 20 Ma but that these systems were not as large as the modern East Antarctic Ice Sheet. Minimal erratic clasts in drifts from the eastern Friis Hills suggest that ice was collecting locally, not being derived from continental-scale glaciations. Dated episodes of downcutting and erosion elsewhere in the Dry Valleys (Lewis et al., 2006, 2007) imply that the ice sheet reached an early maximum configuration about 14 Ma ago. Given this, drifts in the Friis Hills provide important information regarding the earliest formation of the East Antarctic Ice Sheet.

Since downcutting and isolation, surfaces in the eastern Friis Hills have been largely preserved. Alpine glaciers, if they ever formed on the plateau, have left no deposits or they have been eroded without a trace. Evidence exists for only slow subaerial erosion. The volcanic ash, which is preserved just below the ground surface, shows no evidence of chemical weathering. All of this suggests that cold and dry climate conditions extend back to at least 14 Ma. Moreover, climate was probably relatively cold as long ago as 19.76 Ma to prevent rapid devitrification of glass shards in a wet, proglacial environment.

The dated ash deposit in Friis II provides an important constraint on the age of ancient tills in the western Dry Valleys region. The ancient alpine valley segments preserved on Mt Feather, Mt Fleming, and elsewhere have not been dated using radiometric methods. Minimum age estimates from exposure age dating suggest ages older than Pliocene (Bruno et al., 1997; Schäfer et al., 1999) but these estimates are controversial because some tills are reported to contain Pliocene-aged diatoms (Wilson et al., 2008). The

dated stratigraphic sequence in the Friis Hills suggests that these could also be as old as 20 Ma.

- Stacked drifts, each comprised of multiple till sheets and interbeds of outwash, fill an ancient paleovalley in the eastern Friis Hills. These drifts make up a till sequence that is 35 m thick. Measured along the paleovalley axis, from bedrock to bedrock contact, the paleovalley is 570 m long; measured perpendicular to the paleovalley axis it is 675 to 700 m wide. The floor dips 2 to 3 m to the northeast along the axis, which produces a slope of less than 1°.
- The drifts that fill the paleovalley are divided into two groups: Friis and Cavendish drifts. In the field, the two drifts can be divided based on surface morphology, color, and surface clast lithology. Laboratory analyses provided statistical evidence for the division based on sedimentology and clast lithology and texture.
- Tills in Friis drift, at the bottom of the sequence, were deposited from small alpine glaciers. This ice originated in or near the Friis Hills. Tills in Cavendish drift were deposited from a more massive glacial system. These glaciers deposited Cavendish drift in the paleovalley, eventually filling it with ablation tills and proglacial sediments. Glaciers depositing Cavendish drift, either simultaneously or later, cross-cut the paleovalley and eroded previously deposited tills and bedrock.
- Based on striations, tills in Friis drift were deposited by ice flowing at 029°, parallel to the paleovalley's axis. Cross-cutting striations from Cavendish ice are orientated at 099°.
- Nearly *in-situ*, bedded volcanic ash lenses found near the surface of Friis II shows that the valley was cut and the till was deposited 19.76 ± 0.07 Ma ago. Cavendish ice later

deposited a series of thick tills and outwash beds, and crosscut the paleovalley between 19.76 and 14 Ma.

- During the deposition of both Friis and Cavendish drifts (20-14 Ma), the East Antarctic Ice Sheet was smaller than it is today. Evidence comes from the very low percentage of erratics. Friis I and II and Cavendish III are the only units that hold erratic clasts. These erratics are likely from rock sources near the Friis Hills that were then eroded away after 19.76 Ma ago.
- About 14 Ma ago the East Antarctic Ice Sheet expanded, overtopped some drainage divides, and began to erode new valleys. Ice flowed around and over the Friis Hills. Through the process of selective linear erosion it began to cut the trough that now holds Taylor Glacier. The resulting topography redirected ice through low-elevation troughs adjacent to the Friis Hills.
- Taylor drift, a cold-based till, was deposited as the thick East Antarctic Ice Sheet flowed through troughs adjacent to the Friis Hills. This occurred after 14 Ma ago.
- The combination of topographic isolation and persistent cold and dry conditions has protected deposits in the Friis Hills from erosion for millions of years. Deep troughs prevent East Antarctic outlet glaciers from flowing over the Friis Hills. Persistent cold and dry climate conditions have prevented local alpine glaciers from eroding drifts preserved on the plateau surface. At present only subaerial processes affect surfaces in the eastern Friis Hills.
- Preserved plant fossils interbedded in the tills can be used to provide evidence for paleoclimate from the time period prior to and at the beginning of the Mid-Miocene Climate Optimum.

LITERATURE CITED

Allibone, A., Cox, S., Graham, I., Smillie, R., Johnstone, R., Ellery, S., and Palmer, K., 1993, Granitoids of the Dry Valleys area, southern Victoria Land, Antarctica: plutons, field relationships, and isotopic dating: New Zealand Journal of Geology and Geophysics, v. 36, p. 281-297.

Ashworth, A.C., and Lewis, A.R., 2011, The Early Miocene paleoclimate of the McMurdo Dry Valleys region of Antarctica, ISAES, Edinburgh, Scotland.

Balco, G., and Shuster, D.L., 2009, Production rate of cosmogenic ^{21}Ne in quartz estimated from ^{10}Be, ^{26}Al, and ^{21}Ne concentrations in slowly eroding Antarctic bedrock surfaces: Earth and Planetary Science Letters, v. 281, p. 48-58.

Barrett, P.J., 1981, History of the Ross Sea region during the deposition of the Beacon Supergroup 400 – 180 million years ago: Journal of the Royal Society of New Zealand, v. 11, p. 447-458.

Bart, P.J., Anderson, J.B., Trincardi, F., and Shipp, S.S., 2000, Seismic data from the Northern Basin, Ross Sea record multiple expansions of the East Antarctic Ice Sheet during the late Neogene: Marine Geology, v. 166, p. 31-50.

Bartek, L.R., Vail, P.R., Anderson, J.B., Emmet, P.A., and Wu, S., 1991, Effect of Cenozoic ice sheet fluctuations in Antarctica on the stratigraphic signature of the Neogene: Journal of Geophysical Research, v. 96, p. 6753-6778.

Bliss, A.K., Cuffey, K.M., and Kavanaugh, J.L., 2011, Sublimation and surface energy budget of Taylor Glacier, Antarctica: Journal of Glaciology, v. 57, p. 684-696.

Brook, E.J., Kurz, M.D., Ackert, R.P., Jr., Denton, G.H., Brown, E.T., Raisbeck, G.M., and Yiou, F., 1993, Chronology of Taylor Glacier advances in Area Valley, Antarctica, using in situ cosmogenic ^{3}He and ^{10}Be: Quaternary Research, v. 39, p. 11-23.

Boulton, G.S., 1978, Boulder shapes and grain-size distribution of debris as indicators of transport paths through a glacier and till genesis: Sedimentology, v. 25, p. 773-799.

Bruno, L.A., Baur, H., Graf, T., Schlüchter, C., Signer, P., and Wieler, R., 1997, Dating of Sirius Group tillites in the Antarctic Dry Valleys with cosmogenic ^{3}He and ^{21}Ne: Earth and Planetary Science Letters, v. 147, p. 37-54.

Cuffey, K.M., Conway, H., Gades, A.M., Hallet, B., Lorrain, R., Severinghaus, J.P., Steig, E.J., Vaugh, B., and White, J.W., 2000, Entrainment at cold glacier beds: Geology, v. 28, p. 351-354.

DeConto, R.M., and Pollard, P., 2003, Rapid Cenozoic glaciation of Antarctica induced by declining atmospheric CO_2: Nature, v. 421, p. 425-429.

Doran, P.T., McKay, C.P., Clow, G.D., Dana, G.L., Fountain, A.G., Nylen, T., and Lyons, W.B., 2002, Valley floor climate observations from the McMurdo dry valleys, Antarctica, 1986-2000: Journal of Geophysical Research, v. 107, p. 4772-4784.

Dreimanis, A., 1989, Tills: their genetic terminology and classification: Goldthwait, R.P. and Matsch, C.L., ed, Genetic classification of glacigenic deposits, A.A. Balkema, Rotterdam, p. 68-78.

Folk, R.L., 1974, Petrography of Sedimentary Rocks: Austin, Hemphill Publishing Company, p. 15-41.

Gwyn, Q.H.J., and Dreimanis, A., 1979, Heavy mineral assemblages in tills and their use in distinguishing glacial lobes in the Great Lakes region: Canadian Journal of Earth Sciences, v. 16, p. 2219-2235.

Hicock, S.R., Barrett, P.J., and Holme, P.J., 2003, Fragment of an ancient outlet glacier system near the top of the Transantarctic Mountains: Geology, v. 31-39, p. 821-824.

Kjaer, K.H., 1999, Mode of subglacial transport deduced from till properties, Mýrdalsjökull, Iceland: Sedimentary Geology, v. 128, p. 271-292.

Lewis, A.R., Marchant, D.R., Ashworth, A.C., Hedenas, L., Hemming, S.R., Johnsons, J.V., Leng, M.J., Machuls, M.L., Newton, A.E., Raine, J.I., Willenbring, J.K., Williams, M., and Wolfe, A.P., 2008, Mid-Miocene cooling and the extinction of tundra in continental Antarctica: Proceedings of the National Academy of Sciences, v. 105, p. 10676-10680.

Lewis, A.R., Marchant, D.R., Ashworth, A.C., Hemming, S.R., and Machlus, M.L., 2007, Major middle Miocene global climate change: Evidence from East Antarctica and the Transantarctic Mountains: Geological Society of America, Bulletin, v. 119, p. 1449-1461.

Lewis, A.R., Marchant, D.R. Kowalewski, D.E., Baldwin, S.L., and Webb, L.E., 2006, The age and origin of the Labyrinth, western Dry Valleys, Antarctica: Evidence for extensive middle Miocene subglacial floods and freshwater discharge to the Southern Ocean, Geology, v. 34, p. 513-516.

Long Term Ecological Research Network, McMurdo Dry Valleys, 2011, (http://tropical.lternet.edu:8080/knb/metacat?action=read&qformat=lter&insertTemplate=0&docid=knb-lter-mcm.7003.5, [last accessed 1 August, 2011]

Marchant, D.R., Denton, G.H., and Sugden, D.E., 1993, Miocene glacial stratigraphy and landscape evolution of western Asgard Range, Antarctica: Geografiska Annaler, v. 75, p. 303-330.

Miller, K.G., Fairbanks, R.G., and Mountain, G.S., 1987, Tertiary oxygen isotope synthesis, sea-level history, and continental margin erosion: Paleooceanography, v. 2, p. 1-19.

Morgan, D., Putkonen, J., Balco, G., and Stone, J., 2010, Quantifying regolith erosion rates with cosmogenic nuclides ^{10}Be and ^{26}Al in the McMurdo Dry Valleys, Antarctica: Journal of Geophysical Research, v. 115, p. 1-17.

Naish, T.R., Powell, R., Levy, R., and 53 others, 2009, Obliquity-paced Pliocene West Antarctic ice sheet oscillations: Nature, v. 458, p. 322-328.

Naish, T.R., Woolfe, K.J., Barret, P.J., and 30 others, 2001, Orbitally induced oscillations in the East Antarctic Ice Sheet at the Oligocene/Miocene boundary: Earth and Atmospheric Sciences, v. 413 p. 719-723.

NASA Earth Observatory: Terra Nova Bay Polynya, Antarctica. 2007, http://earthobservatory.nasa.gov /IOTD/view.php?id=8134 [last accessed 28 July 2011].

Ruddiman, W., and Raymo, M., 1988, Northern Hemisphere climate regimes during the past 3 Ma: possible tectonic connection: Journal of Royal Society B, v. 318, p. 411-430.

Schäfer, J.M., Ivy-Ochs, S., Wieler, R., Leya, I., Baur, H., Denton, G.H., and Schlüchter, C., 1999, Cosmogenic noble gas studies in the oldest landscape on Earth: Surface exposure ages of the Dry Valleys, Antarctica: Earth and Planetary Science Letters, v. 167, p. 215-226.

Shevenell, A.E., Kennett, J.P., and Lea, D.W., 2008, Middle Miocene ice sheet dynamics, deep-sea temperatures, and carbon cycling: a southern ocean perspective: Geochemistry, Geophysics, Geosystem, v. 9.

Shevenell, A.E., Kennett, J.P., and Lea, D.W., 2004, Middle Miocene southern ocean cooling and Antarctic cyrosphere expansion: Science, v. 305, p. 1766-1770.

Stroeven, A.P., and Prentice, M.L., 1997, A case for Sirius Group alpine glaciation at Mount Fleming, South Victoria Land, Antarctica: A case against Pliocene East Antarctic Ice Sheet reduction: Geological Society of America Bulletin, v. 109-7, p. 825-840.

Sugden, D.E., and John, B.S., 1976, Glaciers and Landscape: London, Edward Arnold, p. 192-202.

Summerfield, M.A., Sugden, D.E., Denton, G.H., Marchant, D.R., Cockburn, H.A.P., and Stuart, F.M., 1999, Cosmogenic isotope date support previous evidence of extremely low rates of denudation in the Dry Valleys region, southern Victoria Land, Antarctica: Geological Society of London, Special Publication, v. 162, p. 255-267.

Willenbring, J.K., Marchant, D.R., Oberholzer, P., Schaefer, J.M., Johnson, J.V., and Lewis, A.R., 2006, Plio-Pliestocene history of Ferrar Glacier, Antarctica: Implications for climate and ice sheet stability: Earth and Planetary Science Letters, v. 243, p. 489-503.

Wilson, G.S., Barron, J.A., Ashworth, A.C., and 20 others, 2002, The Mount Feather Diamicton of the Sirius Group: an accumulation of indicators of Neogene Antarctic glacial and climate history: Palaeogeography, Palaeoclimatology, Palaeoecology, v. 182, p. 117-131.

Zachos, J.C., Dickens, G.R., and Zeebe, R.E., 2008, An early Cenozoic perspective on greenhouse warming and carbon-cycle dynamics: Nature, v. 451, p. 279-283.

Zachos, J.C., Pagani, M., Sloan, L., Thomas, E., and Billups, K., 2001a, Trends, rhythms, and aberrations in global climate 65 Ma to present: Science, v. 292, p. 686-693.

Zachos, J.C., Shackleton, N.J., Revenaugh, J.S., Pälike, H., and Flower, B.P., 2001b, Climate response to orbital forcing across the Oligocene-Miocene boundary: Science, v. 292, p. 274-278.

APPENDIX A. SEDIMENTOLOGY OF TILL SAMPLES

Table A.1. Sedimentological analysis of drift matrix.

Sample	Till unit	Gravel %	Sand %	Mud %	Silt %	Clay %
ASS-10-07	F2	0.00	66.06	33.94	28.72	5.22
ASS-10-09A	F2	49.89	34.71	15.40	13.84	1.57
ASS-10-09B	F2	32.61	48.41	18.97	16.44	2.53
ASS-10-17B	C3	28.61	60.78	10.62	9.72	0.90
ASS-10-23	C3	28.82	59.99	11.19	9.96	1.23
ASS-10-29A	C3	37.39	39.34	23.28	22.09	1.19
ASS-10-29B	C3	34.34	49.70	15.96	14.43	1.53
ASS-10-30A	C3	35.63	51.41	12.96	11.52	1.44
ASS-10-30B	C3	31.58	51.66	16.76	14.70	2.06
ASS-10-32	C2	35.14	56.20	8.65	7.48	1.17
ASS-10-33	C2	39.48	51.05	9.47	8.31	1.16
ASS-10-36	C2	33.41	51.49	15.10	13.49	1.61
ASS-10-38	C2	24.23	62.17	13.61	12.56	1.05
ASS-10-41	F1	57.71	37.33	4.95	4.23	0.72
ASS-10-43A	UD	39.66	50.98	9.36	8.62	0.74
ASS-10-43B	UD	42.72	44.29	12.99	11.22	1.77
ASS-10-46	C2	37.33	48.11	14.57	13.11	1.46
ASS-10-50	C1	35.35	45.30	19.35	18.62	0.73
ASS-10-51	C1	35.30	49.32	15.38	14.48	0.90
ASS-10-53A	F1	30.03	51.55	18.42	17.57	0.86
ASS-10-53B	F1	18.90	70.90	10.19	9.04	1.16
ASS-10-55	F1	35.50	53.68	10.81	10.18	0.64
ASS-10-56	F1	16.04	71.92	12.04	10.70	1.34
ASS-10-58	F1	22.21	68.09	9.71	8.67	1.04
ASS-10-60	C3	24.99	52.53	22.48	20.37	2.11
ASS-10-62A	C3	28.14	57.70	14.16	12.21	1.95
ASS-10-62B	F1	47.25	33.79	18.97	17.53	1.44
ASS-10-64	UD	58.13	37.74	4.13	3.54	0.59
ASS-10-69	C3	26.12	56.72	17.16	15.22	1.94
ASS-10-70	C2	25.57	59.52	14.91	13.35	1.56
ASS-10-73B	C3	36.44	42.88	20.68	19.54	1.15
ASS-10-74A	UD	17.87	64.43	17.69	16.16	1.53
ASS-10-74B	UD	31.95	47.96	20.09	18.79	1.30
ASS-10-81	C3	29.88	53.75	16.37	14.42	1.95
ASS-10-82	F1	40.16	48.69	11.15	9.86	1.29
ALS-08-21	F2	33.99	59.29	6.71	*	*

* = not measured

Table A.1. (continued)

Sample	Till unit	Gravel %	Sand %	Mud %	Silt %	Clay %
ALS-08-22	F2	29.64	56.74	13.62	*	*
ALS-08-23	F2	21.14	69.63	9.19	*	*
ALS-08-39A	F2	23.87	37.10	39.03	37.32	1.71
ALS-08-41	C3	12.86	63.13	24.02	*	*
ALS-08-42	C3	20.27	50.11	29.62	*	*
ALS-08-43	C3	25.36	51.81	22.82	*	*
ALS-08-50a	F2	9.76	65.56	24.68	*	*
ALS-08-50b	F2	10.15	65.47	24.37	*	*
ALS-08-54	F2	25.63	52.28	22.09	*	*
ALS-08-55	F1	31.61	40.94	27.46	*	*
ALS-08-56	F1	56.21	26.63	17.17	*	*

* = not measured

F2=Friis drift lower till unit; F1=Friis drift upper till unit; C1=Cavendish drift upper till unit; C2=Cavendish drift middle unit; C3=Cavendish drift lower unit contains multiple tills; UD=Undifferentiated

Table A.2 Gravel analysis.

Sample	Initial Wt	>16 mm (-4φ)	>8mm (-3φ)	>4mm (-2φ)	>2mm (-1φ)	Pan	Gravel Sum
ASS-10-07	79.29	0.00	0.00	0.00	0.00	79.29	0.00
ASS-10-09A	2018.94	349.60	226.04	217.56	214.03	1011.71	1007.23
ASS-10-09B	1539.45	85.16	69.94	168.88	178.08	1037.39	502.06
ASS-10-17B	2111.19	0.00	141.08	187.43	275.40	1507.28	603.91
ASS-10-23	2177.06	6.55	155.03	225.60	240.23	1549.65	627.41
ASS-10-29A	1726.84	0.00	47.31	260.83	337.44	1081.26	645.58
ASS-10-29B	2261.32	0.00	170.42	270.38	335.83	1484.69	776.63
ASS-10-30A	2482.16	0.00	243.28	345.64	295.42	1597.82	884.34
ASS-10-30B	1878.75	37.56	171.75	168.86	215.10	1285.48	593.27
ASS-10-32	2708.95	0.00	236.95	348.58	366.48	1756.94	952.01
ASS-10-33	2473.46	0.00	246.63	391.88	338.01	1496.94	976.52
ASS-10-36	1998.07	0.00	140.60	196.77	330.14	1330.56	667.51
ASS-10-38	2159.46	0.00	38.54	186.86	297.76	1636.30	523.16
ASS-10-41	2088.19	0.00	477.44	376.82	350.93	883.00	1205.19
ASS-10-43A	2268.17	6.13	261.96	256.63	374.93	1368.52	899.65
ASS-10-43B	1973.47	0.00	252.22	299.90	290.89	1130.46	843.01
ASS-10-46	2168.85	0.00	269.17	267.60	272.80	1359.28	809.57
ASS-10-50	1621.84	0.00	145.47	182.64	245.24	1048.49	573.35
ASS-10-51	2059.67	0.00	177.45	259.56	290.11	1332.55	727.12
ASS-10-53A	1706.20	0.00	86.69	157.51	268.16	1193.84	512.36
ASS-10-53B	1741.53	0.00	44.69	142.65	141.82	1412.37	329.16
ASS-10-55	2163.99	5.56	301.16	250.51	211.08	1395.68	768.31
ASS-10-56	2151.77	0.00	73.13	107.71	164.41	1806.52	345.25
ASS-10-58	2253.77	0.00	87.69	190.39	222.39	1753.30	500.47
ASS-10-60	1952.52	0.00	60.81	190.44	236.75	1464.52	488.00
ASS-10-62A	2244.03	0.00	202.06	212.54	216.96	1612.47	631.56
ASS-10-62B	1852.63	0.00	223.57	391.65	260.06	977.35	875.28
ASS-10-64	2188.80	12.01	394.44	348.13	517.84	916.38	1272.42
ASS-10-69	1948.28	0.00	187.30	143.80	177.80	1439.38	508.90
ASS-10-70	1960.60	0.00	82.52	169.64	249.09	1459.35	501.25
ASS-10-73B	2011.22	0.00	112.18	320.13	300.48	1278.43	732.79
ASS-10-74A	2090.54	0.00	72.54	100.21	200.91	1716.88	373.66
ASS-10-74B	2184.66	0.00	126.26	184.55	387.16	1486.69	697.97
ASS-10-81	1785.32	0.00	126.48	213.60	193.41	1251.83	533.49
ASS-10-82	1890.00	0.00	164.31	252.45	342.27	1130.97	759.03
ALS-08-21	1141.97	0.00	114.91	155.22	118.05	753.79	388.18
ALS-08-22	964.87	0.00	102.40	87.61	95.95	678.91	285.96
ALS-08-23	918.20	0.00	43.41	66.91	83.79	724.09	194.11
ALS-08-39A	574.97	0.00	7.26	43.93	86.05	437.73	137.24

Table A.3. Sand analysis.

Sample	Initial sand and mud split	Weight washed sand	>2 mm (-1φ)	>0.5 mm (1φ)	>0.25 mm (2φ)	>0.125 mm (3φ)	>0.0625 mm (4φ)	Pan	Sand sum
ASS-10-07	79.29	53.75	8.56	8.78	11.25	14.94	8.85	1.33	52.38
ASS-10-09A	98.70	69.14	5.50	9.86	19.11	23.37	10.52	0.73	68.36
ASS-10-09B	95.72	69.50	6.95	15.54	19.89	17.48	8.91	0.73	68.77
ASS-10-17B	91.85	79.31	11.75	15.81	22.08	19.73	8.82	0.71	78.19
ASS-10-23	96.88	82.67	8.86	14.44	22.40	24.29	11.66	0.64	81.65
ASS-10-29A	90.30	58.54	5.06	9.83	12.37	18.32	11.15	1.58	56.73
ASS-10-29B	95.97	73.80	10.09	15.00	16.85	19.07	11.63	1.00	72.64
ASS-10-30A	82.09	66.83	8.20	14.40	17.15	15.51	10.30	1.13	65.56
ASS-10-30B	82.83	64.24	7.32	11.66	16.18	15.97	11.41	1.49	62.54
ASS-10-32	88.51	77.39	12.09	17.21	20.16	17.15	10.09	0.81	76.70
ASS-10-33	95.52	81.39	14.35	18.93	21.17	16.66	9.47	0.80	80.58
ASS-10-36	76.47	54.85	7.73	13.08	16.56	13.40	8.36	0.66	59.13
ASS-10-38	99.41	82.55	6.72	16.07	23.35	22.26	13.16	0.93	81.56
ASS-10-41	70.03	61.96	16.59	20.40	15.44	6.55	2.85	0.20	61.83
ASS-10-43A	96.38	82.14	13.94	18.18	20.30	18.89	10.12	0.68	81.43
ASS-10-43B	97.38	76.33	14.97	18.32	16.95	14.91	10.15	1.40	75.30
ASS-10-46	89.19	70.64	11.53	13.74	15.78	14.97	12.44	2.07	68.46
ASS-10-50	99.53	69.76	8.70	14.04	18.01	16.94	12.05	1.30	69.74
ASS-10-51	73.19	56.55	7.57	12.18	14.14	12.94	8.96	0.89	55.79
ASS-10-53A	84.43	62.94	6.95	11.63	17.76	17.15	8.71	0.71	62.20
ASS-10-53B	88.62	77.98	1.09	2.88	18.61	44.02	10.88	0.54	77.48
ASS-10-55	89.90	75.33	6.60	12.25	22.04	23.29	10.65	0.57	74.83
ASS-10-56	98.97	85.04	5.60	21.54	31.60	21.65	4.39	0.14	84.78
ASS-10-58	97.47	86.84	7.93	15.61	25.62	27.19	8.96	1.51	85.31
ASS-10-60	79.31	55.70	2.80	7.08	15.97	19.38	10.31	0.92	55.54
ASS-10-62A	76.38	62.28	9.48	13.16	14.78	14.28	9.63	1.00	61.33
ASS-10-62B	98.26	65.86	7.58	13.53	15.78	14.64	11.40	2.67	62.93
ASS-10-64	93.36	84.57	20.55	25.37	21.33	11.84	5.06	0.47	84.15
ASS-10-69	99.52	77.84	6.49	10.65	20.87	25.15	13.24	1.47	76.40

Table A.3. (continued)

Sample	Initial sand and mud split	Weight washed sand	>2 mm (-1φ)	>0.5 mm (1φ)	>0.25 mm (2φ)	>0.125 mm (3φ)	>0.0625 mm (4φ)	Pan	Sand sum
ASS-10-70	96.73	78.56	9.65	16.33	19.78	19.03	12.56	1.21	77.35
ASS-10-73B	97.17	66.80	5.67	9.71	17.98	21.09	11.10	1.17	65.55
ASS-10-74A	98.68	78.56	9.74	11.94	20.31	24.02	11.41	1.02	77.42
ASS-10-74B	90.72	64.53	7.90	10.54	16.71	20.31	8.48	0.65	63.94
ASS-10-81	71.33	55.47	3.91	9.12	13.33	18.31	10.01	0.68	54.68
ASS-10-82	95.96	79.01	14.73	21.43	18.81	14.16	8.95	0.76	78.08
ALS-08-21	23.30	20.98	2.95	4.18	6.80	4.90	2.10	0.05	20.93
ALS-08-22	25.00	20.25	2.72	3.15	5.69	5.44	3.16	0.08	20.16
ALS-08-23	24.15	21.95	3.17	4.41	5.36	6.05	2.84	0.12	21.83
ALS-08-39A	104.22	52.29	2.33	6.62	13.73	18.09	10.02	1.52	50.79

Table A.4. Silt analysis.

Sample	Diameter (phi)	Dried weight	Beaker weight	Total sediment weight
ASS-10-07	<0.0625mm (4φ)	29.12	29.03	0.09
	<0.031mm (5φ)	29.27	29.18	0.09
	<0.0156mm (6φ)	29.37	29.29	0.08
	<0.0078mm (7φ)	28.11	28.04	0.07
	<0.0039mm (8φ)	28.02	27.96	0.06
ASS-10-09A	<0.0625mm (4φ)	29.67	29.36	0.31
	<0.031mm (5φ)	29.36	29.27	0.09
	<0.0156mm (6φ)	29.29	29.22	0.07
	<0.0078mm (7φ)	29.10	29.04	0.06
	<0.0039mm (8φ)	29.59	29.53	0.06
ASS-10-09B	<0.0625mm (4φ)	29.59	29.38	0.21
	<0.031mm (5φ)	29.43	29.37	0.06
	<0.0156mm (6φ)	29.60	29.54	0.06
	<0.0078mm (7φ)	29.41	29.35	0.06
	<0.0039mm (8φ)	29.34	29.28	0.06
ASS-10-17A	<0.0625mm (4φ)	28.18	28.05	0.13
	<0.031mm (5φ)	28.09	27.97	0.12
	<0.0156mm (6φ)	28.02	27.94	0.08
	<0.0078mm (7φ)	27.44	27.39	0.05
	<0.0039mm (8φ)	27.31	27.29	0.02
ASS-10-23	<0.0625mm (4φ)	29.71	29.53	0.18
	<0.031mm (5φ)	29.70	29.50	0.20
	<0.0156mm (6φ)	29.39	29.23	0.16
	<0.0078mm (7φ)	28.15	28.04	0.11
	<0.0039mm (8φ)	27.94	27.86	0.08
ASS-10-29A	<0.0625mm (4φ)	29.74	29.40	0.34
	<0.031mm (5φ)	29.65	29.38	0.27
	<0.0156mm (6φ)	29.74	29.55	0.19
	<0.0078mm (7φ)	29.51	29.38	0.13
	<0.0039mm (8φ)	29.41	29.31	0.10
ASS-10-29B	<0.0625mm (4φ)	29.51	29.19	0.32
	<0.031mm (5φ)	29.65	29.40	0.25
	<0.0156mm (6φ)	29.20	29.03	0.17
	<0.0078mm (7φ)	29.30	29.19	0.11
	<0.0039mm (8φ)	29.39	29.30	0.09
ASS-10-30A	<0.0625mm (4φ)	27.53	27.34	0.19
	<0.031mm (5φ)	28.23	28.02	0.21
	<0.0156mm (6φ)	28.33	28.20	0.13
	<0.0078mm (7φ)	27.83	27.72	0.11

Table A.4. (continued)

Sample	Diameter (phi)	Dried weight	Beaker weight	Total sediment weight
	<0.0078mm (7φ)	27.47	27.36	0.11
	<0.0039mm (8φ)	27.36	27.27	0.09
ASS-10-46	<0.0625mm (4φ)	29.58	29.36	0.22
	<0.031mm (5φ)	29.46	29.26	0.20
	<0.0156mm (6φ)	29.35	29.23	0.12
	<0.0078mm (7φ)	29.14	29.05	0.09
	<0.0039mm (8φ)	29.62	29.55	0.07
ASS-10-50	<0.0625mm (4φ)	29.76	29.40	0.36
	<0.031mm (5φ)	29.64	29.39	0.25
	<0.0156mm (6φ)	29.67	29.57	0.10
	<0.0078mm (7φ)	29.45	29.39	0.06
	<0.0039mm (8φ)	29.34	29.31	0.03
ASS-10-51	<0.0625mm (4φ)	27.91	27.68	0.23
	<0.031mm (5φ)	27.15	26.94	0.21
	<0.0156mm (6φ)	27.52	27.39	0.13
	<0.0078mm (7φ)	28.18	28.11	0.07
	<0.0039mm (8φ)	27.71	27.67	0.04
ASS-10-53A	<0.0625mm (4φ)	29.61	29.38	0.23
	<0.031mm (5φ)	29.41	29.33	0.08
	<0.0156mm (6φ)	29.31	29.25	0.06
	<0.0078mm (7φ)	29.10	29.06	0.04
	<0.0039mm (8φ)	29.60	29.58	0.02
ASS-10-53B	<0.0625mm (4φ)	29.35	29.23	0.12
	<0.031mm (5φ)	29.54	29.41	0.13
	<0.0156mm (6φ)	29.13	29.04	0.09
	<0.0078mm (7φ)	29.25	29.20	0.05
	<0.0039mm (8φ)	29.35	29.30	0.05
ASS-10-55	<0.0625mm (4φ)	27.54	27.36	0.18
	<0.031mm (5φ)	28.20	28.05	0.15
	<0.0156mm (6φ)	28.32	28.22	0.10
	<0.0078mm (7φ)	27.79	27.74	0.05
	<0.0039mm (8φ)	27.75	27.72	0.03
ASS-10-56	<0.0625mm (4φ)	29.48	29.24	0.24
	<0.031mm (5φ)	29.65	29.53	0.12
	<0.0156mm (6φ)	29.48	29.37	0.11
	<0.0078mm (7φ)	29.53	29.44	0.09
	<0.0039mm (8φ)	29.70	29.63	0.07
ASS-10-58	<0.0625mm (4φ)	28.13	28.04	0.09
	<0.031mm (5φ)	28.06	27.99	0.07

Table A.4. (continued)

Sample	Diameter (phi)	Dried weight	Beaker weight	Total sediment weight
	<0.0156mm (6φ)	27.99	27.94	0.05
	<0.0078mm (7φ)	27.42	27.38	0.04
	<0.0039mm (8φ)	27.30	27.27	0.03
ASS-10-60	<0.0625mm (4φ)	104.18	103.91	0.27
	<0.031mm (5φ)	108.76	108.62	0.14
	<0.0156mm (6φ)	102.57	102.47	0.10
	<0.0078mm (7φ)	102.87	102.80	0.07
	<0.0039mm (8φ)	100.80	100.74	0.06
ASS-10-62A	<0.0625mm (4φ)	29.78	29.62	0.16
	<0.031mm (5φ)	29.69	29.55	0.14
	<0.0156mm (6φ)	29.49	29.38	0.11
	<0.0078mm (7φ)	29.54	29.45	0.09
	<0.0039mm (8φ)	29.73	29.65	0.08
ASS-10-62B	<0.0625mm (4φ)	27.89	27.72	0.17
	<0.031mm (5φ)	27.17	26.97	0.20
	<0.0156mm (6φ)	27.56	27.41	0.15
	<0.0078mm (7φ)	28.20	28.11	0.09
	<0.0039mm (8φ)	27.71	27.66	0.05
ASS-10-64	<0.0625mm (4φ)	27.44	27.34	0.10
	<0.031mm (5φ)	28.13	28.03	0.10
	<0.0156mm (6φ)	28.29	28.20	0.09
	<0.0078mm (7φ)	27.77	27.70	0.07
	<0.0039mm (8φ)	27.75	27.69	0.06
ASS-10-69	<0.0625mm (4φ)	29.50	29.22	0.28
	<0.031mm (5φ)	29.69	29.41	0.28
	<0.0156mm (6φ)	29.25	29.05	0.20
	<0.0078mm (7φ)	29.36	29.18	0.18
	<0.0039mm (8φ)	29.42	29.30	0.12
ASS-10-70	<0.0625mm (4φ)	29.77	29.53	0.24
	<0.031mm (5φ)	29.75	29.53	0.22
	<0.0156mm (6φ)	29.42	29.24	0.18
	<0.0078mm (7φ)	28.17	28.04	0.13
	<0.0039mm (8φ)	27.96	27.87	0.09
ASS-10-73B	<0.0625mm (4φ)	27.98	27.71	0.27
	<0.031mm (5φ)	27.12	26.98	0.14
	<0.0156mm (6φ)	27.47	27.40	0.07
	<0.0078mm (7φ)	28.15	28.12	0.03
	<0.0039mm (8φ)	27.70	27.67	0.03
ASS-10-74A	<0.0625mm (4φ)	29.63	29.38	0.25

Table A.4. (continued)

Sample	Diameter (phi)	Dried weight	Beaker weight	Total sediment weight
	<0.031mm (5φ)	29.58	29.36	0.22
	<0.0156mm (6φ)	29.74	29.57	0.17
	<0.0078mm (7φ)	29.47	29.37	0.10
	<0.0039mm (8φ)	29.37	29.30	0.07
ASS-10-74B	<0.0625mm (4φ)	29.56	29.20	0.36
	<0.031mm (5φ)	29.73	29.40	0.33
	<0.0156mm (6φ)	29.23	29.03	0.20
	<0.0078mm (7φ)	29.31	29.19	0.12
	<0.0039mm (8φ)	29.39	29.32	0.07
ASS-10-81	<0.0625mm (4φ)	27.92	27.69	0.23
	<0.031mm (5φ)	27.18	26.98	0.20
	<0.0156mm (6φ)	27.56	27.38	0.18
	<0.0078mm (7φ)	28.22	28.09	0.13
	<0.0039mm (8φ)	27.76	27.66	0.10
ASS-10-82	<0.0625mm (4φ)	28.23	28.04	0.19
	<0.031mm (5φ)	28.13	27.96	0.17
	<0.0156mm (6φ)	28.08	27.92	0.16
	<0.0078mm (7φ)	27.45	27.36	0.09
	<0.0039mm (8φ)	27.34	27.26	0.08
ALS-08-39	<0.0625mm (4φ)	30.08	29.50	0.58
	<0.031mm (5φ)	30.04	29.50	0.54
	<0.0156mm (6φ)	29.33	29.22	0.11
	<0.0078mm (7φ)	29.28	29.20	0.08
	<0.0039mm (8φ)	29.46	29.40	0.06

Table B.1. Clast lithology and characterisitics.

Sample	Till Unit	Clast/kg	Dolerite	Granite	Sandstone	Siltstone	Striated	Molded	Polished	Stained	Desert Varnish	Ventifact
ALE-10-07B	F2	0	3	5	0	0	0	3	1	0	0	0
ALE-10-09A	F2	21	34	6	1	0	0	9	2	0	0	0
ALE-10-09B	F2	15	44	4	3	0	1	13	3	0	0	0
ALE-10-17A	C3	15	31	5	0	0	0	3	1	0	0	0
ALE-10-17B	C3	13	27	3	0	0	1	1	2	0	1	0
ALE-10-21	UD	27	34	5	2	0	0	9	1	1	0	0
ALE-10-23	C3	22	29	5	3	1	2	15	4	0	0	0
ALE-10-29A	C3	7	17	1	0	0	0	2	0	0	0	0
ALE-10-29B	C3	14	27	0	0	0	2	9	3	0	0	0
ALE-10-30	C3	25	38	0	0	0	0	12	5	0	0	0
ALE-10-32	C2	34	40	0	3	0	1	14	6	0	0	0
ALE-10-33	C2	27	42	3	0	0	1	15	3	0	0	0
ALE-10-36	C2	24	31	4	4	0	1	22	5	0	0	0
ALE-10-38	C2	13	41	4	1	0	0	18	2	0	0	0
ALE-10-41	F1	69	61	6	1	1	0	20	1	1	0	0
ALE-10-43A	UD	26	42	12	0	0	1	14	5	0	0	0
ALE-10-43B	UD	49	7	46	0	0	0	4	0	0	0	0
ALE-10-46	C2	30	32	8	0	0	1	9	1	0	0	0
ALE-10-50	C1	17	38	7	1	0	0	16	1	0	0	0
ALE-10-51	C1	21	41	4	2	0	0	12	0	0	0	0
ALE-10-53A	F1	11	32	6	0	0	4	10	1	0	0	0
ALE-10-55	F1	43	34	2	9	0	0	12	0	0	0	0
ALE-10-56	F1	21	29	0	8	0	0	1	0	1	0	0
ALE-10-58	F1	8	28	0	2	0	0	6	0	1	0	0
ALE-10-60	C3	5	32	11	5	0	2	21	3	3	0	0
ALE-10-62A	C3	31	41	0	0	0	0	10	0	0	0	0

Table B.1. (continued)

Sample	Till Unit	Clast/kg	Dolerite	Granite	Sandstone	Siltstone	Striated	Molded	Polished	Stained	Desert Varnish	Ventifact
ALE-10-62B	F1	18	42	0	0	0	0	11	0	2	0	0
ALE-10-64	UD	68	46	25	1	0	2	23	1	3	0	0
ALE-10-69	C3	26	37	0	0	0	0	2	0	0	0	0
ALE-10-70	C2	22	38	0	0	0	0	12	1	2	0	0
ALE-10-73	C3	2	11	1	2	0	1	3	0	0	0	0
ALE-10-74	UD	12	27	19	1	0	0	9	0	1	0	0
ALE-10-81	C3	15	21	13	5	0	0	8	0	0	0	0
ALE-10-82	F1	19	37	1	0	0	0	5	2	1	0	0
ALS-08-21	F2	30	31	0	1	0	0	11	0	2	0	0
ALS-08-22	F2	33	44	0	0	0	0	13	1	0	0	0
ALS-08-23	F2	21	43	0	0	0	0	4	0	0	0	0
ALS-08-39A	F2	3	14	32	3	1	0	7	0	0	0	0
ALS-08-39B	F2	3	15	1	3	0	0	10	0	0	0	0
ALS-08-41	C3	7	45	6	2	2	0	7	0	0	1	0
ALS-08-42	C3	24	53	4	1	1	3	18	2	0	0	0
ALS-08-43	C3	26	51	2	0	0	0	6	0	0	0	0
ALS-08-50a	F2	7	21	21	7	0	0	10	2	0	1	0
ALS-08-50b	F2	3	41	1	4	0	0	10	0	0	1	0
ALS-08-54	F2	20	42	7	3	0	0	13	0	0	0	0
ALS-08-55	F1	19	44	1	1	0	0	4	0	0	0	0
ALS-08-56	F1	33	46	2	1	0	0	7	0	0	0	0

F2: Fris drift lower till unit; F1: Fris drift upper till unit; C1: Cavendish drift upper till unit; C2: Cavendish drift middle unit; C3: Cavendish drift lower unit contains multiple; tills; UD: Undifferentiated

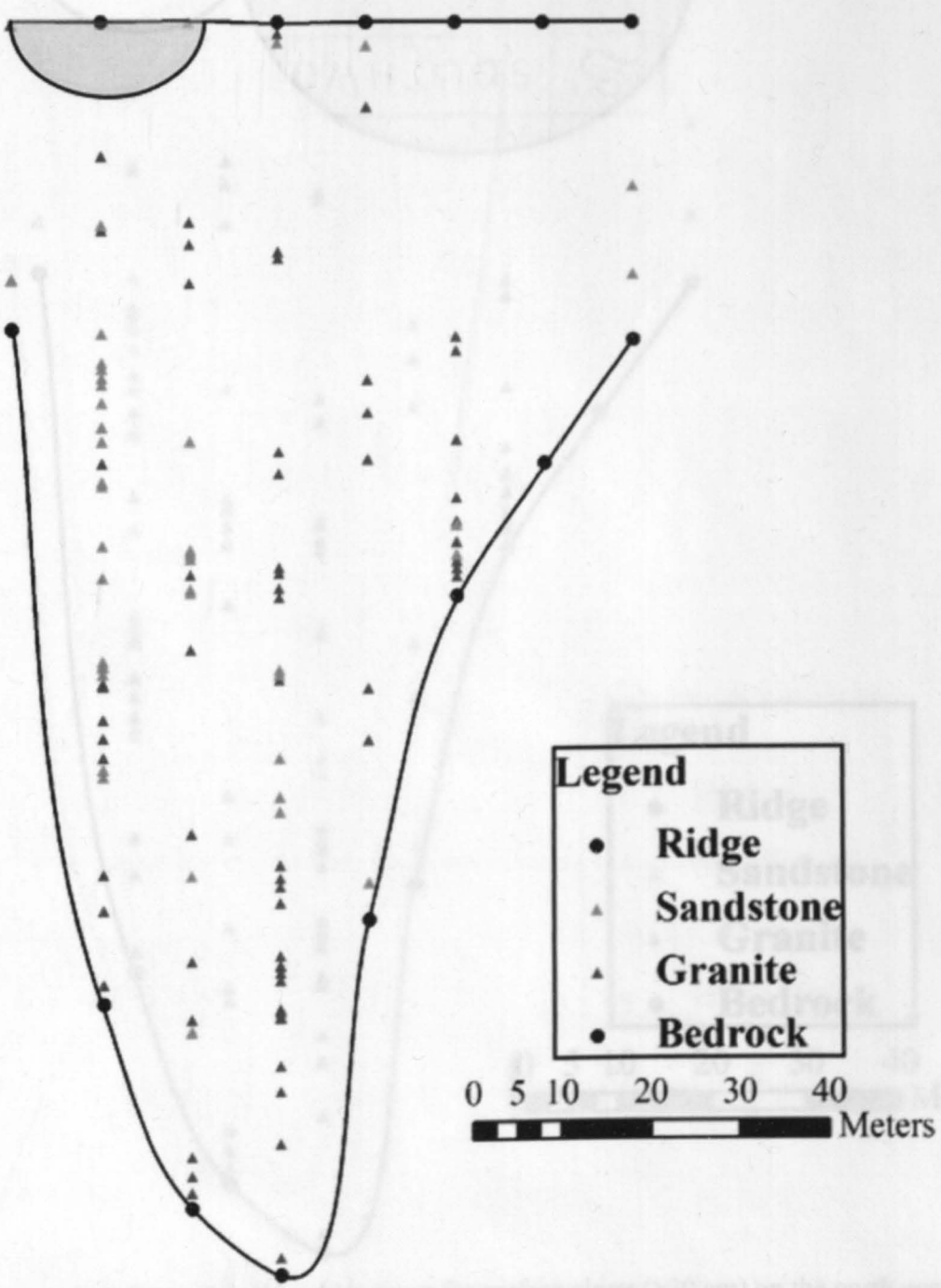

Figure C.1. Cavendish I boulder count for surface clasts (>30 cm) on the north-eastern slope of paleovalley. Diagram shows view to the southwest. Upper line is ridge crest of valley-fill; lower line is the valley-fill bedrock contact. Cavendish I is highlighted in gray.

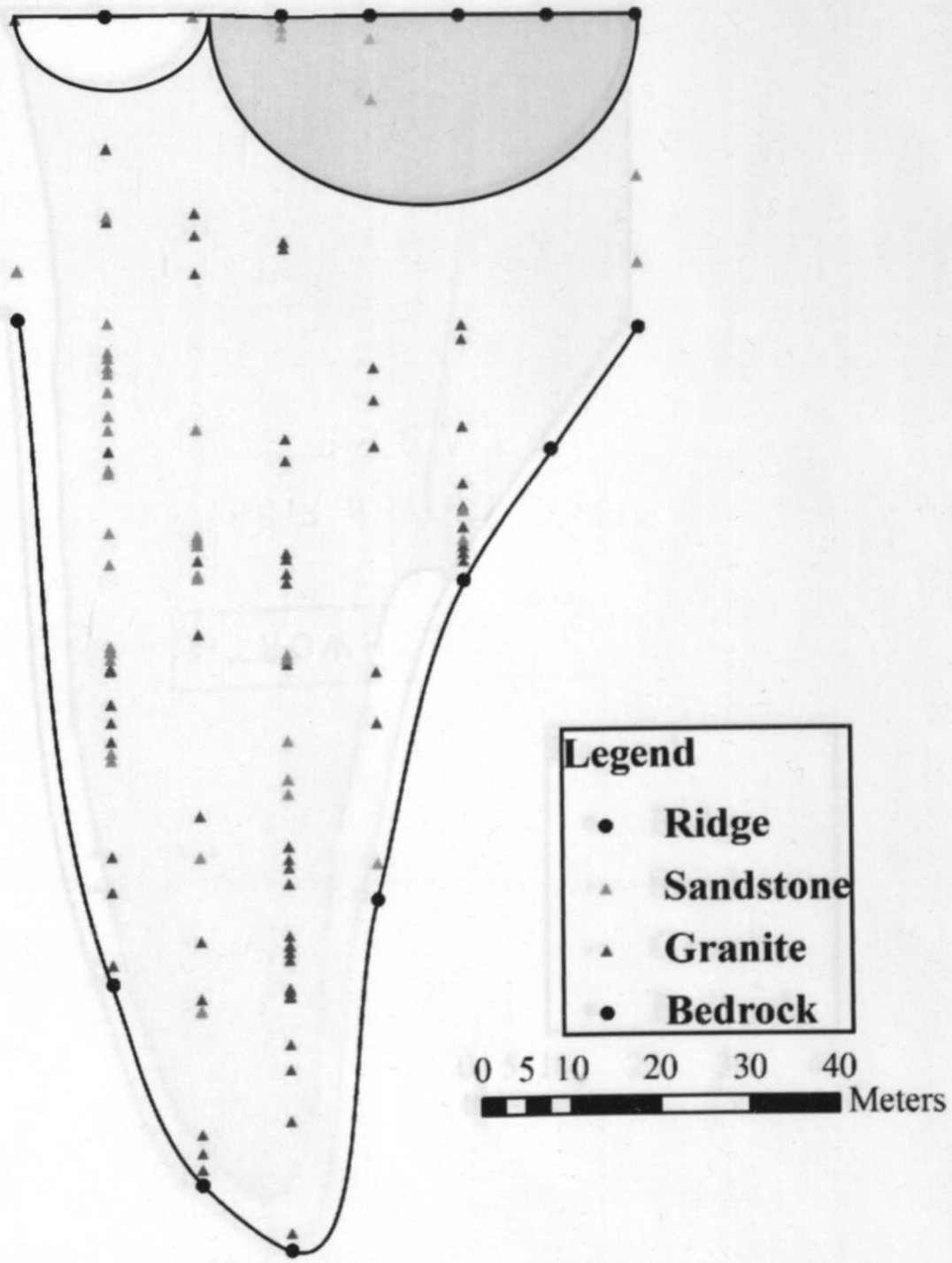

Figure C.2. Cavendish II boulder count for surface clasts (>30 cm) on the north-eastern slope of paleovalley. Diagram shows view to the southwest. Upper line is ridge crest of valley-fill; lower line is the valley-fill bedrock contact. Cavendish II is highlighted in gray

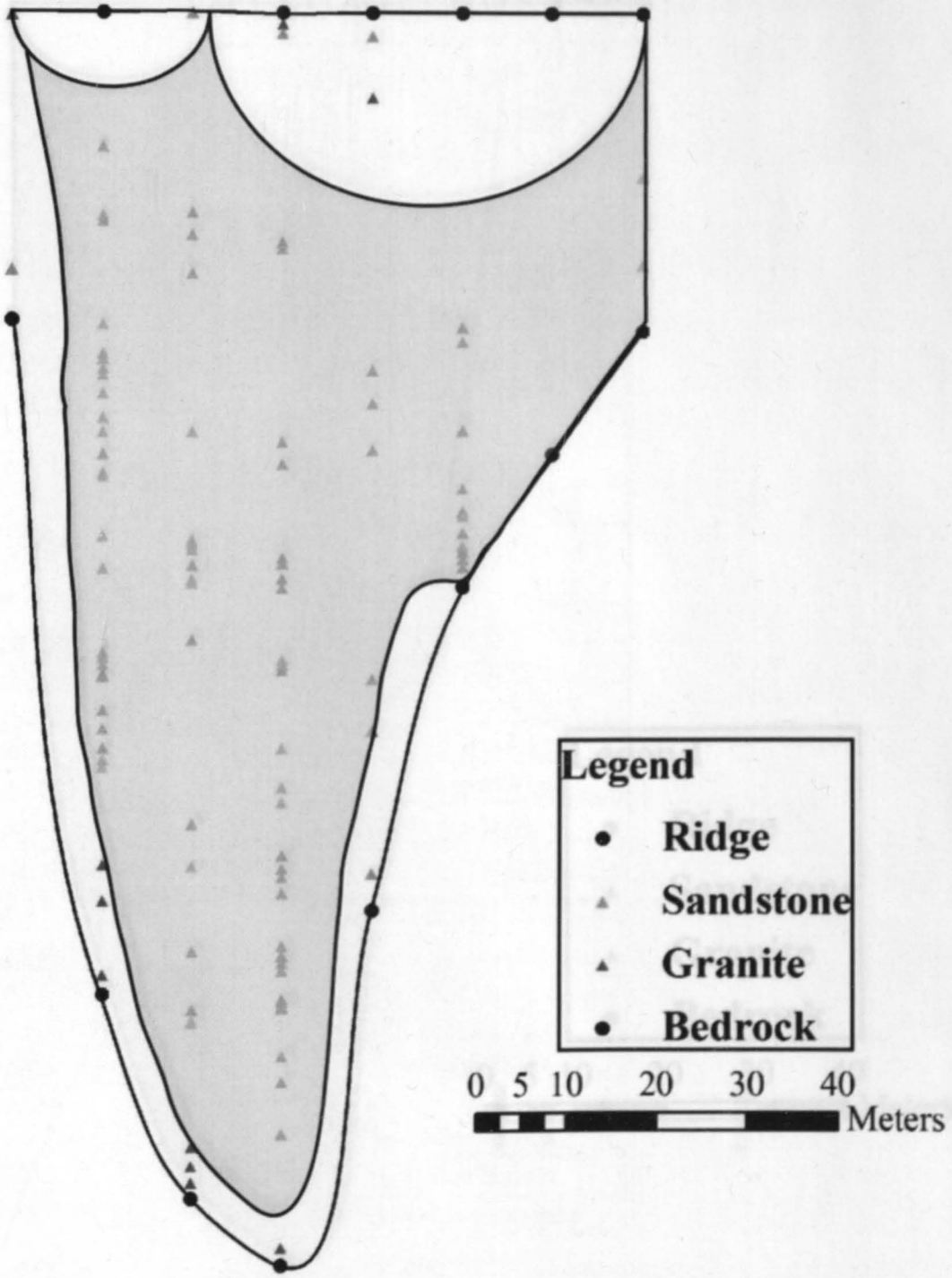

Figure C.3. Cavendish III boulder count for surface clasts (>30 cm) on the north-eastern slope of paleovalley. Diagram shows view to the southwest. Upper line is ridge crest of valley-fill; lower line is the valley-fill bedrock contact. Cavendish III is highlighted in gray.

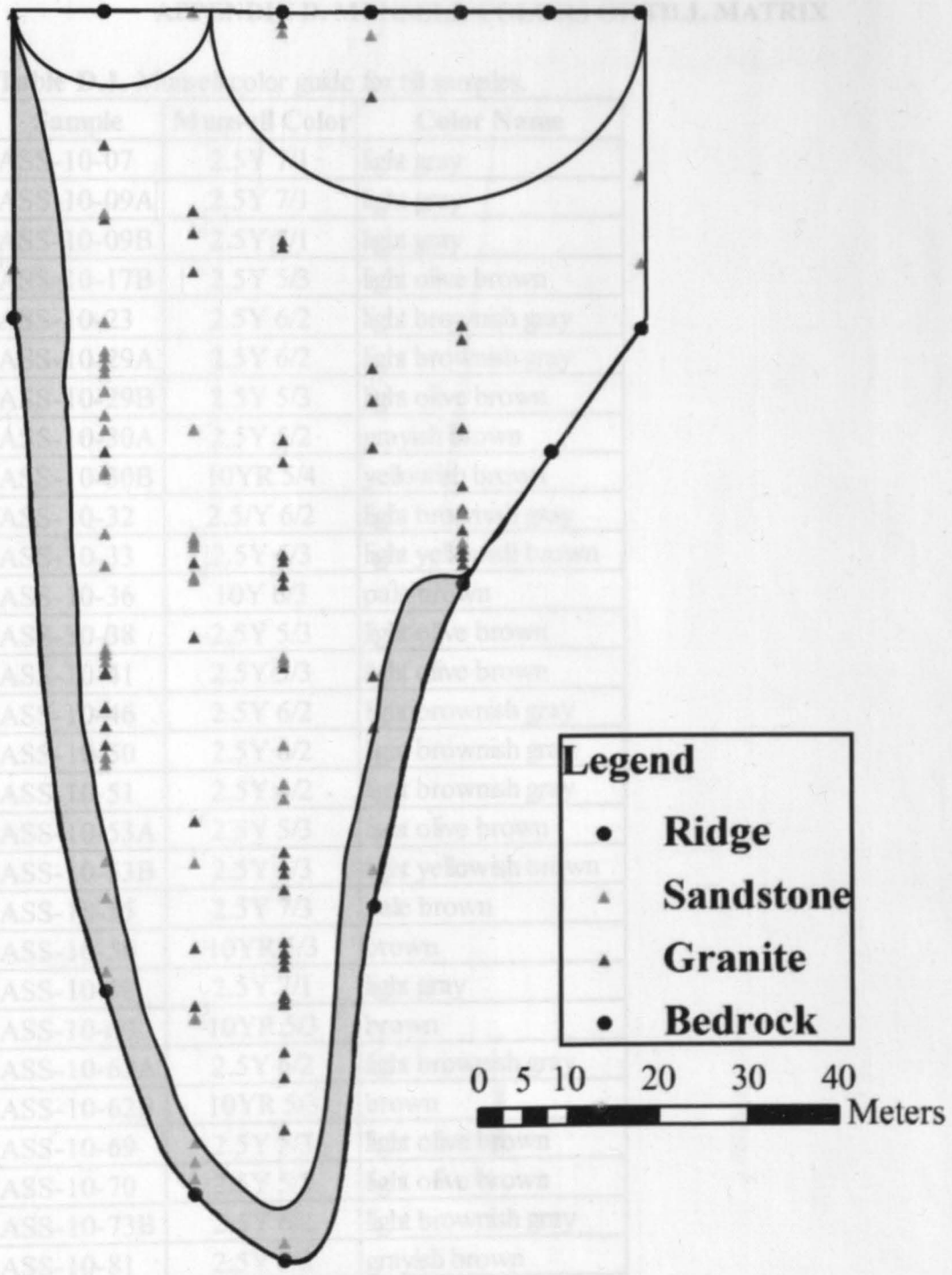

Figure C.4. Friis I boulder count for surface clasts (>30 cm) on the north-eastern slope of paleovalley. Diagram shows view to the southwest. Upper line is ridge crest of valley-fill; lower line is the valley-fill bedrock contact. Friis I is highlighted in gray

APPENDIX D. MUNSELL COLORS OF TILL MATRIX

Table D.1. Munsell color guide for till samples.

Sample	Munsell Color	Color Name
ASS-10-07	2.5Y 7/1	light gray
ASS-10-09A	2.5Y 7/1	light gray
ASS-10-09B	2.5Y 7/1	light gray
ASS-10-17B	2.5Y 5/3	light olive brown
ASS-10-23	2.5Y 6/2	light brownish gray
ASS-10-29A	2.5Y 6/2	light brownish gray
ASS-10-29B	2.5Y 5/3	light olive brown
ASS-10-30A	2.5Y 5/2	grayish brown
ASS-10-30B	10YR 5/4	yellowish brown
ASS-10-32	2.5/Y 6/2	light brownish gray
ASS-10-33	2.5Y 6/3	light yellowish brown
ASS-10-36	10Y 6/3	pale brown
ASS-10-38	2.5Y 5/3	light olive brown
ASS-10-41	2.5Y 5/3	light olive brown
ASS-10-46	2.5Y 6/2	light brownish gray
ASS-10-50	2.5Y 6/2	light brownish gray
ASS-10-51	2.5Y 6/2	light brownish gray
ASS-10-53A	2.5Y 5/3	light olive brown
ASS-10-53B	2.5Y 6/3	light yellowish brown
ASS-10-55	2.5Y 7/3	pale brown
ASS-10-56	10YR 5/3	brown
ASS-10-58	2.5Y 7/1	light gray
ASS-10-60	10YR 5/3	brown
ASS-10-62A	2.5Y 6/2	light brownish gray
ASS-10-62B	10YR 5/3	brown
ASS-10-69	2.5Y 5/3	light olive brown
ASS-10-70	2.5Y 5/3	light olive brown
ASS-10-73B	2.5Y 6/2	light brownish gray
ASS-10-81	2.5Y 5/2	grayish brown

APPENDIX E. DUNCAN GROUPING

Table E.1. Duncan Grouping for significantly different drift characteristics. Alpha 0.10

Characteristic	Till Unit	Samples	Mean	Duncan Group
Gravel	CII	6	32.527	A
	CIII	14	28.602	AB
	FI	10	35.562	AB
	FII	10	23.668	B
Sand	CII	6	54.757	A
	CIII	14	52.965	A
	FI	10	50.352	A
	FII	10	55.525	A
Mud	CII	6	12.718	B
	CIII	14	18.434	AB
	FI	10	14.087	B
	FII	10	20.8	A
Clast/kg	CII	6	25	A
	CIII	14	16.571	AB
	FI	9	26.778	A
	FII	11	14.182	B
Dolerite	CII	6	37.333	A
	CIII	14	32.857	A
	FI	9	39.222	A
	FII	11	30.182	A
Granite	CII	6	3.167	A
	CIII	14	3.643	A
	FI	9	2	A
	FII	11	7	A
Sandstone	CII	6	1.333	A
	CIII	14	1.286	A
	FI	9	2.444	A
	FII	11	2.273	A
Striated	CII	6	0.666	A
	CIII	14	0.785	A
	FI	9	0.444	A
	FII	11	0.091	A
Molded	CII	6	15	A
	CIII	14	8.357	B
	FI	9	8.44	B
	FII	11	9.364	B
Polished	CII	6	3	A
	CIII	14	1.428	B
	FI	9	0.444	B
	FII	11	0.818	B